Not Being (Super)Thin or Solid is Hard: A Study of Grid Hamiltonicity

Esther M. Arkin* Sándor P. Fekete† Kamrul Islam‡ Henk Meijer§‡
Joseph S. B. Mitchell* Yurai Núñez-Rodríguez‡ Valentin Polishchuk¶‖
David Rappaport‡ Henry Xiao‡

November 21, 2008

Abstract

We give a systematic study of Hamiltonicity of grids—the graphs induced by finite subsets of vertices of the tilings of the plane with congruent regular convex polygons (triangles, squares, or hexagons). Summarizing and extending existing classification of the usual, "square", grids, we give a comprehensive taxonomy of the grid graphs. For many classes of grid graphs we resolve the computational complexity of the Hamiltonian cycle problem. For graphs for which there exists a polynomial-time algorithm we give efficient algorithms to find a Hamiltonian cycle.

We also establish, for any $g \geq 6$, a one-to-one correspondence between Hamiltonian cycles in planar bipartite maximum-degree-3 graphs and Hamiltonian cycles in the class $\mathcal{C}_g$ of *girth-g* planar maximum-degree-3 graphs. As applications of the correspondence, we show that for graphs in $\mathcal{C}_g$ the Hamiltonian cycle problem is NP-complete and that for any $N \geq 5$ there exist graphs in $\mathcal{C}_g$ that have exactly N Hamiltonian cycles. We also prove that for the graphs in $\mathcal{C}_g$, a Chinese Postman tour gives a $(1 + \frac{8}{g})$-approximation to TSP, improving thereby the Christofides ratio when $g > 16$. We show further that, on any graph, the tour obtained by Christofides' algorithm is not longer than a Chinese Postman tour.

Keywords: Hamiltonian Cycle, Grid Graph, High-Girth Graph, Covering Tour

*Applied Math and Statistics, Stony Brook University, USA.
†Computer Science, Braunschweig University of Technology, Germany.
‡Computer Science, Queen's University, Canada.
§Roosevelt Academy, The Netherlands.
¶Helsinki Institute for Information Technology, Finland.
‖Corresponding author. Email: valentin.polishchuk@helsinki.fi. Tel: +358-9-191 51239. Fax: +358-9-191 51120.

1 Introduction

Grid computations are at the core of a large variety of algorithms in computer graphics, numerical analysis, computational geometry, robotics, and other fields. The main role played by grids in computer science is to approximate a continuous domain with a discrete point set and/or a graph. Grids are also of theoretical importance, because many results in combinatorics, design and analysis of algorithms, graph theory, and other disciplines use grids as "testbeds". One particular example of such usage is the Hamiltonian Cycle Problem (HCP). The computational complexity of the problem for general graphs was established in the seminal paper of Karp [29]. The NP-completeness of HCP in grid graphs was proved a decade later [27, 28, 34]. Hamiltonicity of grid graphs has been the subject of extensive research [2, 4, 27, 28, 34, 41], including several theses [9, 10, 15, 17, 42].

Usually, the term *grid graph* refers to the *square grid* — the grid defined by a subset of the integer lattice (the vertices of the tiling of the plane with unit squares). *Triangular'grids* are defined by a subset of vertices of the tiling with equilateral triangles; they are a special class of (triangular) "mesh", a structure commonly used in applications (e.g., graphics). Finally, *hexagonal grids* arise from tilings of regular hexagons. Triangular grids and hexagonal grids have received far less study than square grids. In this paper we study all three classes of grid graphs. Table 1 summarizes our results, as well as some prior results, on the HCP in grid graphs. The exact definitions of "thin", "superthin", "polygonal', and "solid" are given in Section 2 below.

1.1 Hamiltonicity and Girth

The *girth* of a graph is the length of the shortest cycle in it. As with other NP-complete problems, a lot of effort has been devoted to establishing "simplest" classes of graphs for which the HCP remains NP-hard. The classical result in this direction is the hardness of the problem in planar cubic graphs [20] (a graph is *cubic* if every vertex has degree exactly 3). Another important step, also taken in [20], is establishing that the HCP in planar cubic graphs remains hard even if restricted to graphs of girth as high as 5. In this paper we extend this result by showing that the problem remains hard in planar graphs of arbitrary girth $g \geq 6$. Since the maximum possible girth of a planar *cubic* graph is 5, instead of considering cubic graphs, we restrict our attention to planar graphs of *maximum* degree 3 (having all vertices with degrees ≤ 3).

Existence of multiple Hamiltonian cycles has been the subject of extensive research too, see [24, Chapter 4] for a survey. Sufficient conditions on the degrees of the vertices of a graph are known, under which the graph, if Hamiltonian at all, contains more than one Hamiltonian cycle: any vertex has odd degree [39], any vertex has the same degree $r > 48$ [21], maximum degree is bounded from below [25], the degree of any vertex in a part of a bipartite graph is at least 3 [40] (and, in general, the number of Hamiltonian cycles is at least exponential in the maximum degree [40]). Thomassen [40] also considered bipartite graphs of large girth, and, as a counterpart to the above results, showed that in a Hamiltonian *cubic* graph (or when one of the two parts has each vertex of degree 4) the number of Hamiltonian cycles increases (at least) exponentially as a function of girth. All of these conditions bound the minimum/maximum degree of the graph vertices from below and do not restrict the graph to be planar. Also, the number of the Hamiltonian cycles is

Grid	Triangular	Square	Hexagonal
General	$\mathcal{NPC}$, **Thm. 3.1**	$\mathcal{NPC}$ [11,34]	$\mathcal{NPC}$**, Thm. 5.4**
Degree-bounded	deg$\leq$ 4: $\mathcal{NPC}$, **Thm. 3.3**	deg$\leq$ 3: $\mathcal{NPC}$ [11,34]	deg$\leq$ 2: $\mathcal{P}$
Thin	$\mathcal{NPC}$, **Cor. 3.2**	$\mathcal{NPC}$, **Obs. 2.4**	
Superthin		$\mathcal{P}$, **Thm. 4.2**	$\mathcal{P}$, **Cor. 5.7**
Polygonal	$\mathcal{P}$, **Thm. 3.8**		$\mathcal{NPC}$**, Cor. 5.5**
Solid	$\mathcal{P}$, **Cor. 3.9**	$\mathcal{P}$ [41]	

Table 1: Hardness of the Hamiltonian cycle problem in grids. See Section 2 for definitions of the grid classes. Our results are in bold. The blanks correspond to open problems.

only estimated. Here we show that for any $g \geq 6, N \geq 5$ there exist planar graphs of girth g with maximum degree 3, having *exactly* N Hamiltonian cycles.

Other related work includes [31], where Hamiltonian cycles in torical grids are considered, and works of Bjorklund and Husfeldt [8], Gabow [18], and Feder and Motwani [16], who showed that "long" cycles can be found in graphs that have "very long" cycles.

Our Contributions

To the best of our knowledge, this paper is the first to address Hamiltonicity of different kinds of grids in full generality[1]. Refer to Table 1. We also give several results on Hamiltonian cycles in high-girth graphs. The following list summarizes our results.

- In Section 2 we define various types of grid graphs, note some relations between them, and make preliminary observations about their Hamiltonicity.
- In Section 3 we prove that the HCP in triangular grid graphs is NP-complete. The grid used in the reduction is thin, which implies NP-completeness of the problem in thin triangular grids. Further, we show that the problem remains NP-complete even if restricted to grids with maximum degree 4. We prove that, except for one counterexample, any polygonal triangular grid without local cut vertices is Hamiltonian.
- In Section 4 we prove that in a superthin square grid there exists at most one Hamiltonian cycle, and that the HCP in superthin square grids is polynomially-solvable.
- In Section 5 we prove that the HCP in hexagonal grid graphs is NP-complete. The grid used in the reduction is polygonal, which implies NP-completeness of the problem in polygonal hexagonal grids. We show that in a superthin hexagonal grid there exists at most one 2-factor. This implies that there is a polynomial-time algorithm for the HCP in superthin hexagonal grids.

[1] In [5, 26, 36] we announced results from Sections 3, 5, 6; [22, 23, 33] independently obtained results, similar to some of ours from Section 3.

- In Section 6 we prove that for $g \geq 6$, the HCP is NP-complete for planar graphs of maximum degree 3 and girth g. We also prove that for any integer $N \geq 5$ there exist planar graphs of maximum degree 3 and girth g that have exactly N Hamiltonian cycles. We show that the TSP in planar graphs of maximum degree 3 and girth g has a $(1+\frac{8}{g})$-approximation given by computing an optimal Chinese Postman tour. We prove that in *any* graph the tour produced by Christofides' algorithm is always of length at most that of a Chinese Postman tour.

Our proofs of Hamiltonicity are constructive and imply efficient algorithms for computing Hamiltonian cycles when they exist.

2 Grids Taxonomy

We first recall some definitions related to (square) grid graphs and introduce some new notions. We then extend the definitions to triangular and hexagonal grids.

Induced graphs. Throughout the paper we will be concerned with graphs "induced" by finite point sets. We say that a graph $G = (V, E)$ is *induced* by a set $S \subset \mathbb{R}^2$ if the vertices of G are the points in S, and the edges of G connect the vertices that are at distance 1; i.e., $V = S$, $E = \{\{i, j\} \mid i, j \in S, |i - j| = 1\}$. To avoid trivialities, all graphs are assumed to be connected and have no degree-1 vertices.

Definition 2.1. *Let $\mathbb{Z}_\square \equiv \mathbb{Z}^2$ be the infinite square (integer) lattice, i.e., the set of vertices of the tiling of $\mathbb{R}^2$ with unit squares. A* square grid graph*, or* square grid*, is a plane graph induced by a subset of vertices of $\mathbb{Z}_\square$.*

Similarly we define triangular and hexagonal grids:

Definition 2.2. *Let $\mathbb{Z}_\triangle$ (resp., $\mathbb{Z}_\hexagon$) be the vertices of the tiling of the plane with unit-side equilateral triangles (resp., regular hexagons). A* triangular grid graph*, or* triangular grid*, (resp.,* hexagonal grid graph*, or* hexagonal grid*) is a plane graph induced by a subset of vertices of $\mathbb{Z}_\triangle$ (resp., $\mathbb{Z}_\hexagon$).*

We use the general term *grid graph*, or simply *grid*, to refer to any of the three types of grid graphs described above.

We define a *pixel* as a grid graph that is a simple cycle of minimal length; simple cycles of length three, four, and six are pixels in the triangular, square, and hexagonal grids, respectively. In the following X denotes the (infinite) set of all pixels of a certain type of lattice. (Note that we use the term "pixel" to denote the *boundary* of a tile – triangle, square, or hexagon.)

Holes. Let $G = (V, E)$ be a grid graph. A bounded face that contains a lattice point in its interior is called a *hole*. We denote by h the number of holes in G.

Let C_0 be the closed walk that separates a grid graph $G = (V, E)$ from its unbounded face. We call C_0 the *outer boundary* of G. Let $C_1, \ldots, C_h$ be the boundaries of the holes; each boundary is a cycle in G. Let $B = \{C_0, C_1, \ldots, C_h\}$ be the *boundary* of G (see Figures 2, 3, and 4). A vertex

$v \in V$ is called *boundary* if it belongs to a boundary cycle. The non-boundary vertices are called *internal*. Note that in a triangular grid a vertex is boundary if and only if its degree is less than 6; a square (resp., hexagonal) grid may have boundary vertices of degree 4 (resp., 3).

Solid Grids. A grid graph is called *solid* if it has no holes; i.e., if every bounded face is a pixel. See Figures 2, 3, and 4 for examples of solid grid graphs.

Umans and Lenhart [41] proved that the Hamiltonian cycle problem is polynomially solvable for solid square grids. Solid square grids were introduced as a discrete analog of simple rectilinear polygons [4, 41].

Cuts and Local Cuts. A vertex $v \in V$ is called a *cut* if its removal disconnects G. Vertex v is a *local cut* if v is a cut or if the number of holes in $G \setminus v$ is less than the number of holes in G; i.e., removal of a local cut "merges" holes. Because a solid grid has no holes, it has no local cuts.

Polygonal Grids. A polygonal grid is a grid with no local cut.

It will be useful to characterize polygonal grids as an assembly of a collection of pixels.

Proposition 2.3. *Let $G = (V, E)$ be a polygonal grid. G can be defined as the union of a set of pixels $\chi \subset X$ such that V is the union of the vertices of pixels in χ and E is the union of the edges of pixels in χ.*

Proof. We take χ as the set of pixels with the following property: for any pixel $p \in \chi$ all edges (and hence – all vertices) of p are in G. We prove that every vertex and every edge of G is contained in at least one pixel from χ.

Indeed, consider a vertex $v \in V$. Since G is connected, there is a vertex $u \in V$ such that $uv \in E$ (Figure 1). Suppose that both pixels (call them p_1 and p_2) that have uv as an edge are not in χ. Then p_i has a vertex a_i such that $a_i \notin V$, $i = 1, 2$. Now, if a_1, a_2 belong to different holes (or one of them belongs to a hole and the other to the unbounded face) of G, then removal of v decreases the number of holes in G. On the other hand, if both a_1, a_2 belong to the same hole (or to the unbounded face), then there is an a_1-a_2 path γ that does not intersect any edge of G (here, γ is a path in the plane, not a path in G). Let G' be the part of G lying within the cycle a_1-u-a_2-γ-a_1; the part is not empty because it contains v. Removal of u disconnects G' from the rest of G, and thus u is a cut – a contradiction.

Similarly, if there is an edge of G that is not an edge of at least one pixel from χ, then one of the edge's incident vertices is a local cut. □

In light of the above proposition, we can say that for every polygonal graph G there exists a set of pixels $\chi \subset X$ that *defines* G.

Dual Grids. Let G be a polygonal grid and let χ be the set of pixels that defines G. The *dual grid* of G is a graph whose vertices are the pixels of χ. The edges of the dual grid connect two vertices if the corresponding pixels share an edge (see Figure 5). The dual grid is a subgraph of

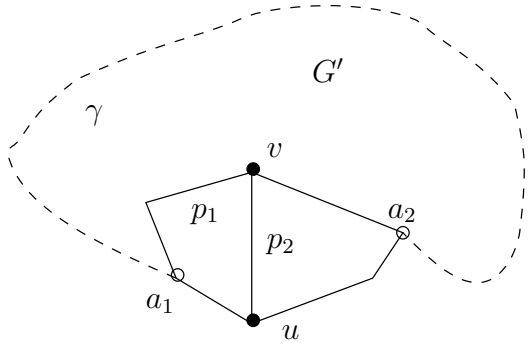

Figure 1: Either removal of v decreases the number of holes, or u is a cut.

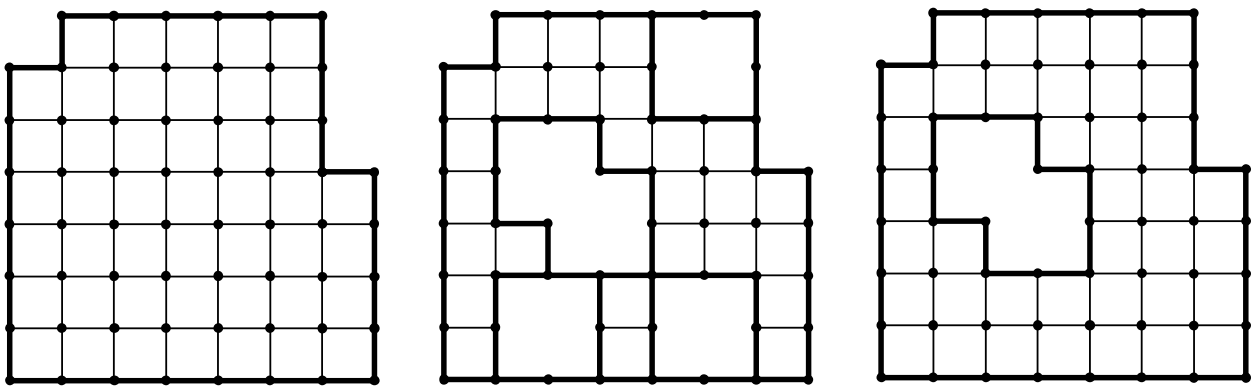

Figure 2: Example square grids: solid (left), with holes (middle), and polygonal (right). Thick lines mark the boundary.

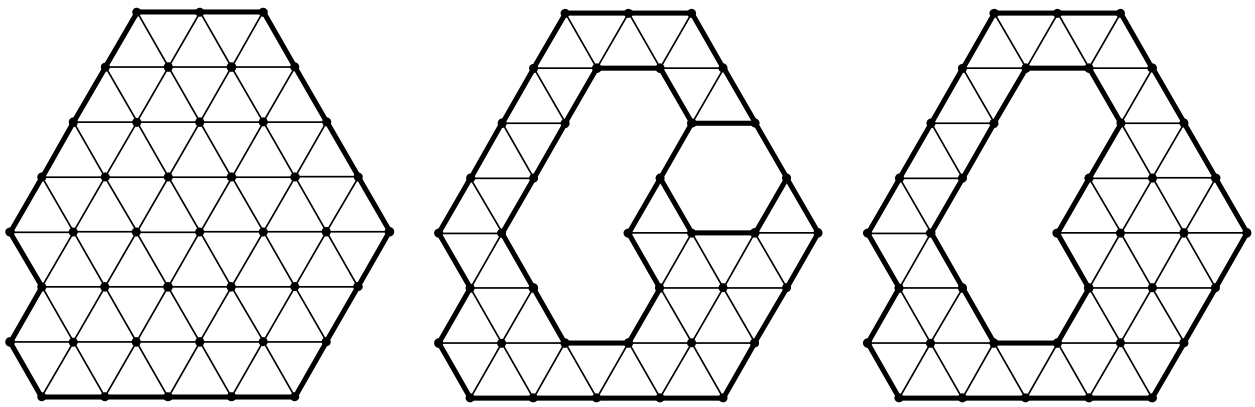

Figure 3: Example triangular grids: solid (left), with holes (middle), and polygonal (right). Thick lines mark the boundary.

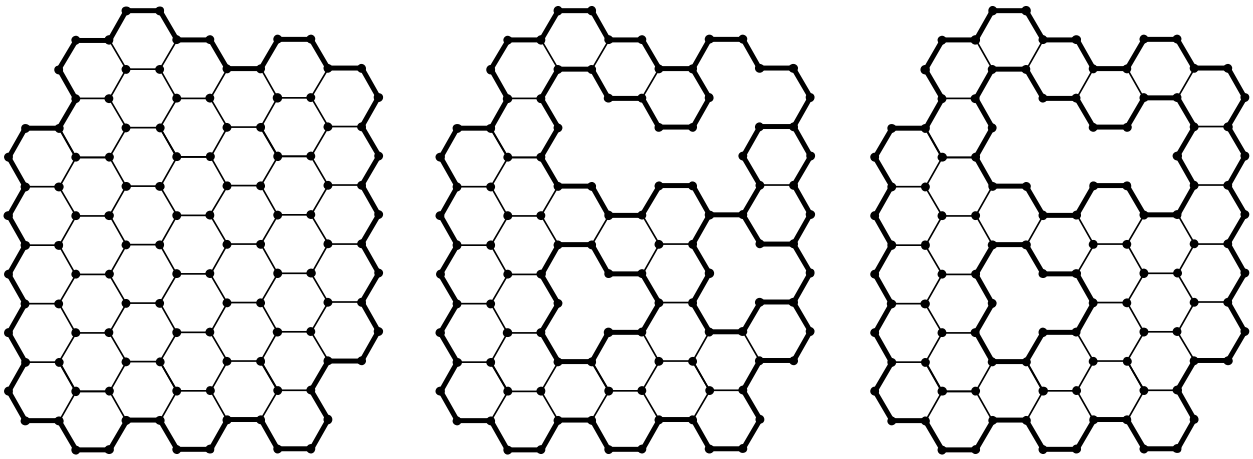

Figure 4: Example hexagonal grids: solid (left), with holes (middle), and polygonal (right). Thick lines mark the boundary.

the graph-theoretic dual of G. We assume that the vertices of the dual grid are embedded at the centers of the faces defined by the corresponding pixels.

Remark. The dual grid of a polygonal square grid is a square grid, the dual grid of a polygonal triangular grid is a hexagonal grid, and the dual grid of a polygonal hexagonal grid is a triangular grid. Notice that in the triangular and hexagonal cases the distances between adjacent vertices in the dual are not equal to one, but, upon scaling, can be assumed to be grid graphs.

Thin Grids. A polygonal grid is called *thin* if all of its vertices are boundary vertices (see Figure 7). Equivalently, a thin grid does not have a "window" (Figure 6) as an induced subgraph.

Superthin Grids. The dual grid of a thin grid is a *superthin* grid. Equivalently, a superthin grid is a grid that contains no pixels (Figure 7). Every vertex of a superthin grid is a local cut.

Degree-Bounded Grids. A grid is called *subcubic* if the maximum degree of a vertex in it is 3. Papadimitriou and Vazirani [34] proved that the Hamiltonian cycle problem on square grids is NP-complete, even when restricted to subcubic grids; Buro [11] gave an alternative proof. If a square grid is subcubic, it does not have a "window" (Figure 6, left) as an induced subgraph; hence, a subcubic square grid is thin.

Observation 2.4. *The Hamiltonian cycle problem on thin square grids is NP-complete.*

A triangular grid is called *subquartic* (resp., *subcubic*) if the maximum degree of a vertex in it is 4 (resp., 3). We do not have any results specific to triangular grids with maximum degree 5, so we do not introduce a name for such grids.

All hexagonal grids are subcubic, and Hamiltonicity of a graph with maximum degree 2 is trivial. Hence, we do not introduce names for degree-bounded hexagonal grids.

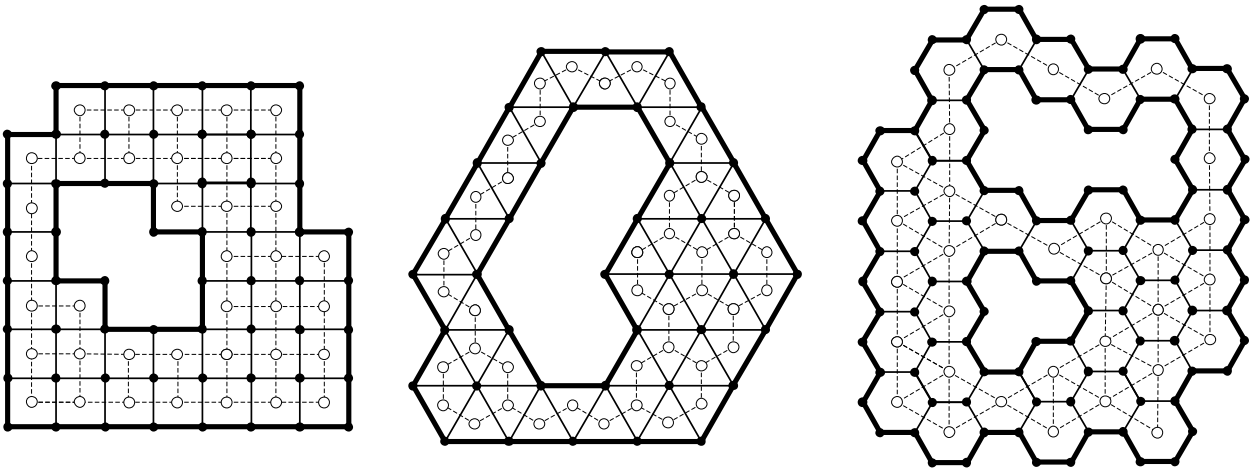

Figure 5: Example dual grids: square (left), triangular (middle), and hexagonal (right). Thick lines mark the boundary. The polygonal grids are represented with solid circles and solid lines. The dual grids are represented with hollow circles and dashed lines.

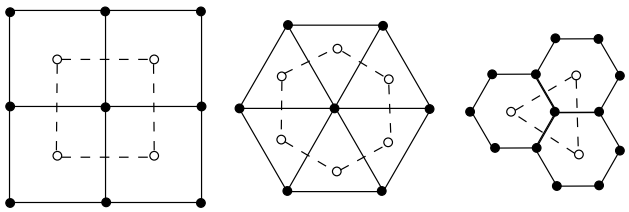

Figure 6: Forbidden subgraphs of thin grids. The duals are the forbidden subgraphs of superthin grids.

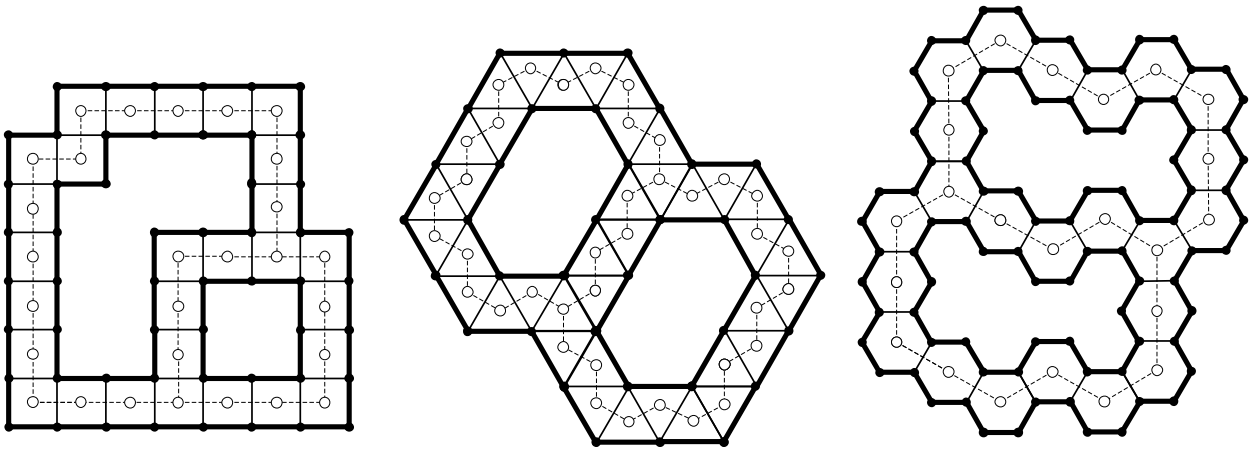

Figure 7: Thin grids and their (superthin) duals: square (left), triangular (middle), and hexagonal (right). Thick lines mark the boundary. The polygonal grids are represented with solid circles and solid lines. The dual grids are represented with hollow circles and dashed lines.

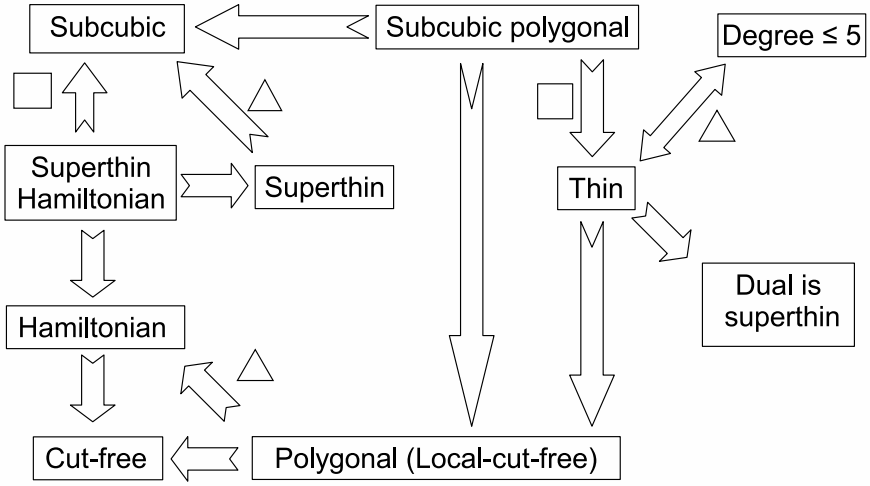

Figure 8: Relationships among grid classes. The relations specific to triangular (resp., square) grids are marked with triangles (resp., squares).

2.1 Summary

The relationships among different classes of grids is shown in Figure 8. Of course, a hexagonal grid is also a superthin triangular grid, but we think that the former is an important enough special case of the latter to be considered separately.

3 Hamiltonian Cycles in Triangular Grids

In this section we show that the HCP for triangular grids is NP-complete, even if the maximum degree of the grid is 4. Next we prove that a polygonal triangular grid is (almost) always Hamiltonian.

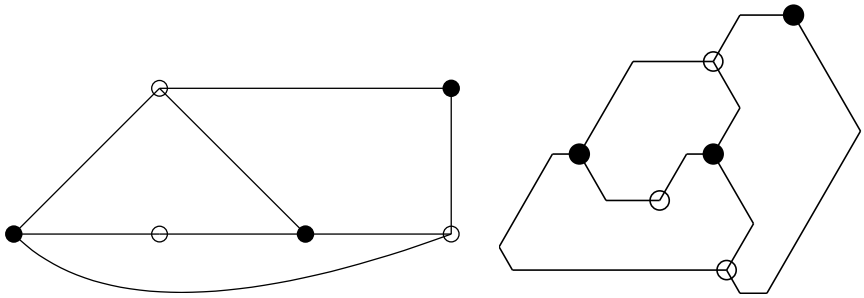

Figure 9: G' and the embedding.

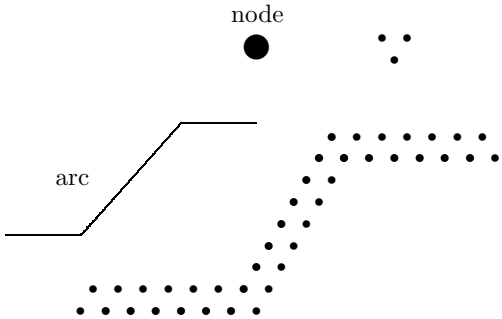

Figure 10: The gadgets.

HCP for Triangular Grids is NP-complete

Itai et al. [27] and Papadimitriou and Vazirani [34] proved that the HCP in square grid graphs is NP-complete by a reduction from HCP in undirected planar bipartite graphs with maximum degree 3 [27]. We follow the idea of [27, 34] to show that the HCP in triangular grids is NP-complete.

Let G' be an undirected planar bipartite graph with maximum degree 3; let the nodes of G' be 2-colored "black" and "white". We say that G' has *nodes* and *arcs*, saving the terms *vertices* and *edges* for the triangular grid graph G that we build from G' as follows. First, G' is embedded in the plane, with the arcs drawn as polygonal paths having segments at angles 0, 60, or 120 degrees with respect to the x-axis, so that the turn angles are 120° at each corner along an embedded polygonal arc (Figure 9). The embedding is then represented by a triangular grid graph G with nodes and arcs simulated by the gadgets shown in Figure 10.

In detail, the nodes are represented by unit triangles; the arcs are simulated by "tentacles". The triangles corresponding to the black (resp., white) nodes of G' are called black (resp., white). A tentacle arc is connected to the black triangle with a "pin" connection (Figure 11, left) and to the white triangle with an "arm" connection (Figure 11, right); the terms are borrowed from [34].

The only means of traversing a tentacle is either by a *return* path (Figure 12, left) or by a (kind of a) *cross* path (Figure 12, right). Of course, there may be many different cross paths, but the

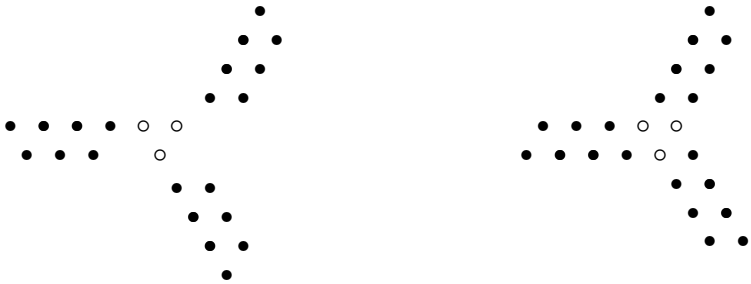

Figure 11: A "pin" connection (left) and an "arm" connection (right). The node gadgets are shown with hollow circles.

Figure 12: The paths.

essential difference between the return and the cross paths is that the former connect the tentacle vertices aligned along a line, while the latter "jump back and forth" between the two lines that bound the tentacle. The idea of the difference is that a cross path connects the two node gadgets at its ends, while a return path just traverses the vertices in the tentacle, returning to the same end from which it started.

Theorem 3.1. *The HCP for triangular grid graphs is NP-complete.*

Proof. If G' has a Hamiltonian cycle, then G has one that traverses the black and white triangles of G in the order of the corresponding arcs of G' in the cycle. It traverses by cross paths the tentacles that correspond to arcs in the cycle. The remaining tentacles are picked up by return paths from the adjacent white triangles.

Conversely, any Hamiltonian cycle $\mathcal{C}$ of G comes from a Hamiltonian cycle of G' in this way. Indeed, it is not hard to see, by inspection of Figure 11, that in $\mathcal{C}$ any triangle, representing a node of G', is attached to exactly two cross paths. □

Observe that the grid in the proof of the above theorem is thin. Thus,

Corollary 3.2. *The HCP for thin triangular grids is NP-complete.*

Subquartic Triangular Grids

Papadimitriou and Vazirani [34] also proved that the HCP in square grid graphs is NP-complete, even when restricted to graphs of maximum degree 3; Buro [11] gave an alternative proof. In this section we prove that the HCP in triangular grids is NP-complete, even when restricted to grids of maximum degree 4.

The graph G constructed in the proof of Theorem 3.1 has certain vertices of degree 5, namely, the vertices of the white triangles and the inner points of the angles of the tentacles. Figure 13

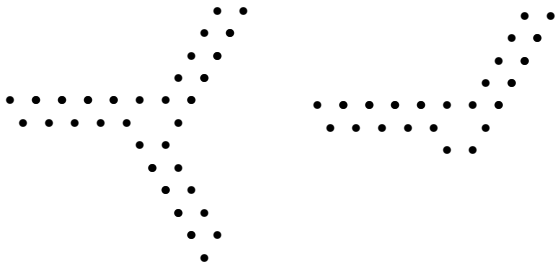

Figure 13: Left: Modified white triangle. Right: Modified turn of a tentacle.

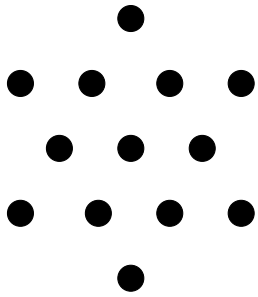

Figure 14: The only non-Hamiltonian polygonal triangular grid graph: the Star of David.

shows how the construction may be modified so that the resulting graph has vertices of degree 4 or less.

Theorem 3.3. *The HCP for subquartic triangular grids is NP-complete.*

Polygonal Triangular Grids are Hamiltonian

The above proof of the hardness of the HCP in triangular grids relied on the grid having local cuts, e.g. the "black" ends of the tentacles, at the "pin" connections (Figure 10, right). It turns out that having local cuts is crucial for the hardness of the problem: we prove below that the HCP is polynomial in triangular grids *without* local cuts. In fact, the connectivity of a triangular grid is so high that, with the exception of one particular graph (which we call the "Star of David", Figure 14), all triangular grids without local cuts are Hamiltonian.

Arkin, Fekete, and Mitchell [4] gave algorithms to construct short covering tours through *square* grids without local cuts, both for solid grids and for grids with holes. Inspired by the ideas from [4], in [36] we gave an algorithm to find a Hamiltonian cycle in a solid triangular grid. The algorithms for solid grids [4,36] take the cycle C around the boundary of (the unbounded face of) the grid, and attach to it all internal vertices. The algorithm for square grids with holes [4] takes the boundary cycles in B and merges them at a low cost (with few additional edges). In this section we extend the ideas from [4,36] to the case of triangular grids *with* holes (but without local cuts). The crucial observations are the following:

1. One can attach to the cycles in B all internal vertices at the cost of 1 per vertex. This results in a cycle cover of G in which the cycles are (vertex-)disjoint.

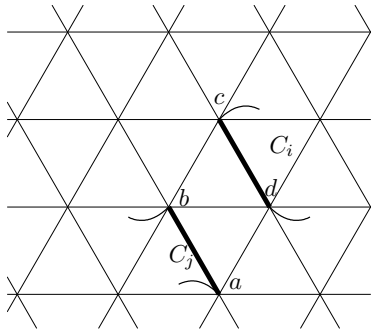

Figure 15: Cycles C_i and C_j face each other: they can be spliced together by flipping the opposite edges of the rhombus *abcd*.

2. A cover of G by vertex-disjoint cycles may be modified so that for any cycle C_i there exists a cycle C_j, "facing" C_i (Figure 15). By "flipping" the edges of the unit rhombus, to which C_i, C_j belong, the cycles may be merged; thus, all the cycles can be spliced into one Hamiltonian, cycle through G.

We formalize and prove these observations in the next two lemmas.

Lemma 3.4. *Let V_6 be the set of internal (degree 6) nodes of G. Then, unless G is the Star of David, the cycles in B can be modified, through a sequence of local modifications, into a set of cycles that visit all vertices in V_6. The cost of the modification is 1 additional edge per vertex of V_6.*

Proof. We modify B by consistently applying three types of local modifications, which we call the L-, V- and Z-modifications. Let $B' = \{C', C'_1, \ldots, C'_h\}$ be the cycles at any particular stage of the modification; we maintain the invariant that C' is a simple cycle within G such that all of the vertices of G that have not been visited by the cycles in B' (i.e., $V \setminus C' \setminus C'_1 \ldots \setminus C'_h$) are inside C'. Each modification adds one new vertex to a cycle in B'. The V-modification is applied only when L cannot be applied; the Z-modification is applied only when no other modification can be applied. The modifications are "monotone" in that each modification will result in B' visiting a superset of the vertices that it previously visited.

We now describe the modifications. Let $v \in V_6 \setminus B'$ be an unvisited vertex. The L-modification is applied as long as there exists a unit equilateral triangle *abv* such that *ab* is an edge of a cycle in B' (Figure 16). The V-modification is applied only when L cannot be applied and B' goes around v as in Figure 17, left; the modified B' is shown in Figure 17, right. Finally, the Z-modification is applied only when none of L, V can be applied and B' goes around v as in Figure 18, left; the modified B' is shown in Figure 18, right.

Let $u \in B'$ be a vertex visited by a cycle in B'. We say that u is a *blunt* (resp., *sharp*) *wedge* if B' makes a 120° (resp., 60°) turn at u.

We now proceed to showing that all vertices in V_6 can be attached to B' as claimed. Suppose that at some stage none of the modifications L, V, or Z can be applied, but B' does not yet go through all vertices in V_6. Then, since G is connected, there exists a vertex $v \in V_6 \setminus B'$ such that

Figure 16: The L-modification. v is the hollow circle.

Figure 17: The V-modification. v is the hollow circle.

at least one of the neighbors of v (say, u) is a vertex of B'. Observe that the degree of v in G is 6, for otherwise v is a boundary vertex and a cycle in B has been going through v from the very beginning.

Since L cannot be applied, none of the edges of the hexagon that "surrounds" v is in B' (Figure 19, left). Since u is in B', at least one of the edges 1,2 in Figure 19, left, must be in B'. Since L cannot be applied, at least one of the vertices adjacent to both v and u must be in B' (say, the edge 1 in Figure 19, left, is in B', so the vertex s is in B' (Figure 19, right)).

Consider three cases:

Case I: s is a sharp wedge like in Figure 20, left. Then V can be applied to attach v to B' (Figure 20, right).

Case II: s is a sharp wedge like in Figure 21, left. Then Z can be applied to attach v to B' (Figure 21, right).

Case III: s is a blunt wedge (Fig 22, left). Then, since L cannot be applied, the vertex t (Figure 22, right), adjacent to both v and s, is in B'.

Now, by considering the same three cases of how B' goes through t, one can conclude that, unless t is a blunt wedge (Case III), v can be attached to B' at a cost of 1 edge. But if t is a blunt

Figure 18: The Z-modification. v is the hollow circle.

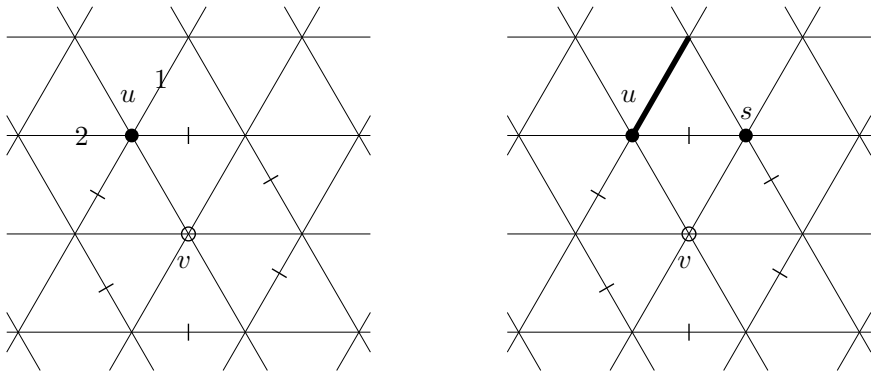

Figure 19: Left: None of the crossed edges may be in B'. At least one of the edges 1,2 (say, 1) is in B'. Right: Thus, $s \in B'$.

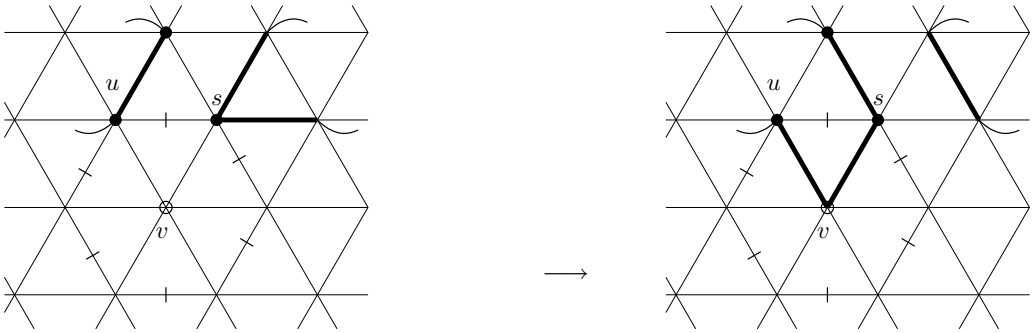

Figure 20: s is a sharp wedge, and a V may be applied.

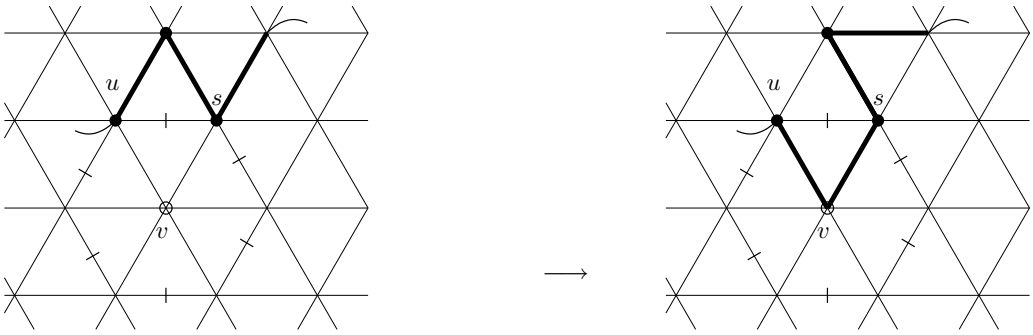

Figure 21: s is a sharp wedge, and a Z may be applied.

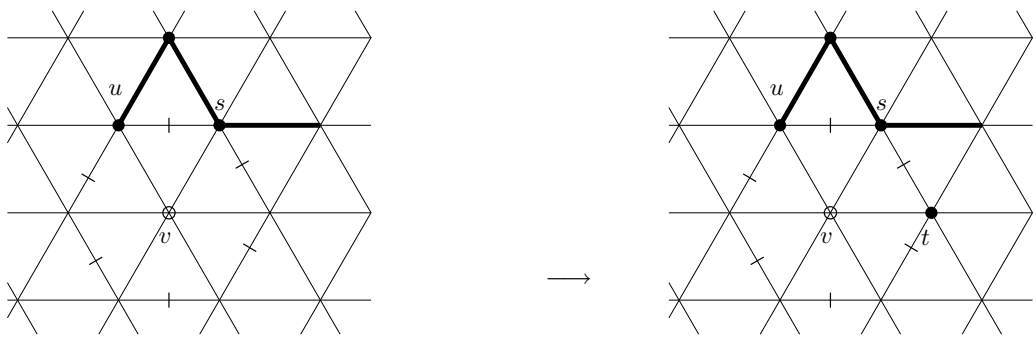

Figure 22: Left: s is a blunt wedge. Right: Thus, $t \in B'$, for otherwise L could be applied.

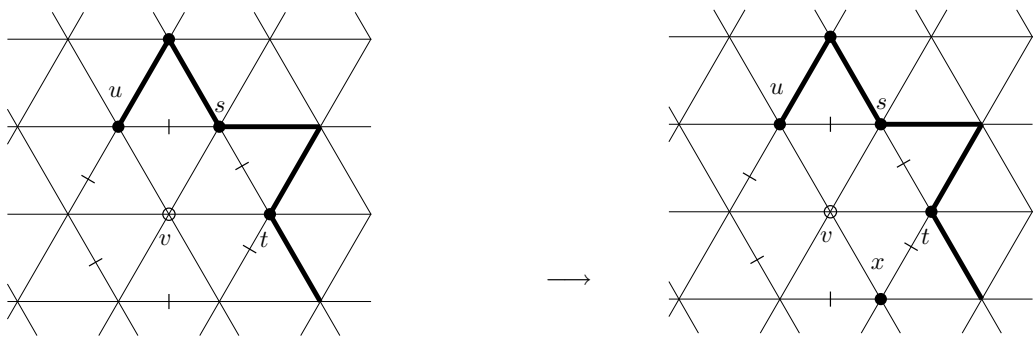

Figure 23: Left: t is a blunt wedge. Right: Thus, $x \in B'$, for otherwise L could be applied.

wedge (Figure 23, left), then, since L cannot be applied, the vertex x, adjacent to both v and t, is in B' (Figure 23, right). Considering the three cases of how B' goes through x, we conclude that x is a blunt wedge too, the vertex, adjacent to both v and x is in B', and is also a blunt wedge. Continuing, we see that if v cannot be attached to B' at a cost of 1, the part of B' that goes around v is one cycle, C, which is the boundary of the Star of David. Since v is a vertex of G, the cycle C does not surround a hole in G; thus, C is the outer boundary of G, and G is the Star of David. □

An interesting corollary of the above lemma is that G admits a cycle cover by *vertex-disjoint* cycles.

Corollary 3.5. *Let G be a triangular grid graph without local cuts. Then, unless G is the Star of David, G admits a cycle cover such that the total length of all cycles in it is equal to the number of vertices of G.*

We prove now that any cycle cover of G by vertex-disjoint cycles can be spliced together into one Hamiltonian cycle through G. We do it by showing that the cycle cover may be modifiedby local modifications into another cycle cover in which there exist two cycles that "face" each other.

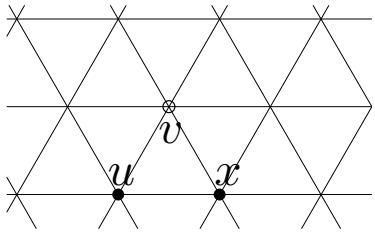

Figure 24: $u \in C_i$, $v \in C_j$. $x \in G$.

Definition 3.6. *Let C_i, C_j be two cycles in G. We say that C_i, C_j* face *each other if there exists a unit rhombus $abcd$, $a, b, c, d \in V$ with $ab \in C_i$, $cd \in C_j$ (see Figure 15).*

Lemma 3.7. *Let B be a set of vertex-disjoint cycles going through all vertices of G. Then there exist two cycles in B that can be modified into cycles that face each other.*

Proof. Because G is connected, there must exist two vertices, u and v, adjacent in G, belonging to different cycles, say $u \in C_i$, $v \in C_j$. Since G is local-cut-free, one of the nodes of the grid adjacent to both u and v must be in G (Figure 24). In other words, there must exist a unit equilateral triangle uvx within G whose vertices are visited by more than one cycle in B.

Consider two cases:

Case I: *One of the edges of the triangle belongs to a cycle in B (Figure 25, left).* Suppose that $ux \in C_i$, $v \in C_j$. If any of the crossed edges in Figure 25, left, is in B, then the cycles C_i and C_j already face each other without any modifications; thus, assume that the crossed edges are not in B. This leaves only two edges of G that could be adjacent to v in B (Figure 25, center). This implies that if any of the edges shown crossed in Figure 25, center, are in B, then C_i and C_j face each other; thus, assume that the crossed edges are not in B.

For v not to be a local cut, at least one of the vertices of the grid that are at distance 1 from v and are on the same horizontal line as v must be in G; suppose, without loss of generality, that it is a vertex w to the right of v (Figure 25, right). If B goes through w as in Figure 26, left, a Z-modification may be applied to C_j to have C_i and the modified C_j face each other (Figure 26, center). So, we may assume that the crossed edges in Figure 26, right, are not in B. Let us consider how B may go through w.

Suppose that B goes through w as in Figure 27, left or Figure 27, center. If $w \in C_k \neq C_i$, then C_i and C_k already face each other; thus, suppose that $w \in C_i$. Then the modifications as in Figure 28, left and Figure 28, center, lead to modified C_i and C_j facing each other. Finally, if B goes through w as in Figure 27, right, a modification as in Figure 28, right, leads to the desired result.

Case II: *None of the edges of the triangle belongs to a cycle in B.* In other words, u, v, x belong to different cycles, say C_u, C_v, C_x. If one of the edges, crossed in Figure 29, left, is in B, then we are in Case I; thus, suppose that none of the crossed edges is in B. This leaves for each of u, v, x only two edges of the grid that are possibly adjacent to the vertex in B (Figure 29,

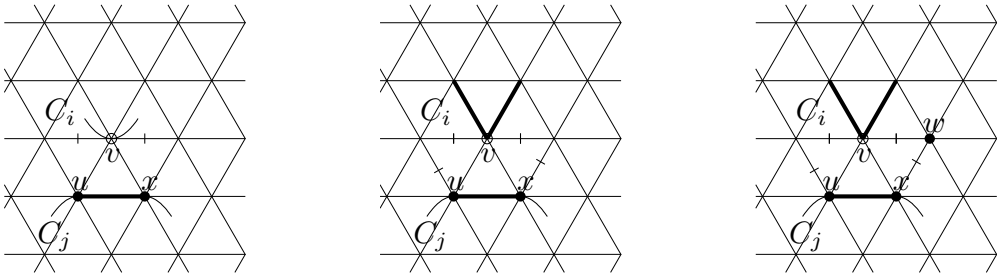

Figure 25: Left: $ux \in C_i$, $v \in C_j$, crossed edges are not in B. Center: the edges of C_j adjacent to v may be deduced; crossed edges are not in B. Right: $w \in G$.

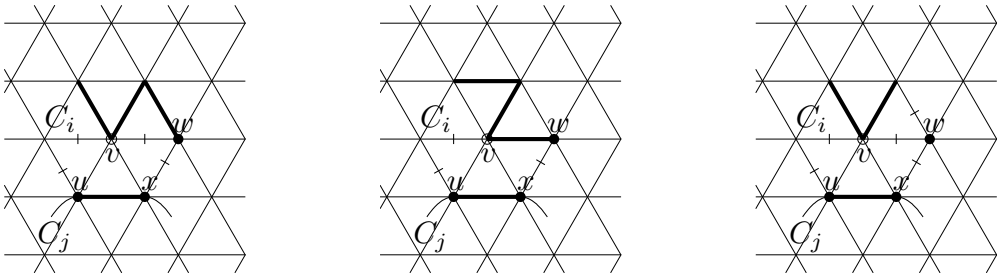

Figure 26: Left and center: A Z leads to the cycles facing each other. Right: Assuming all crossed edges are not in B.

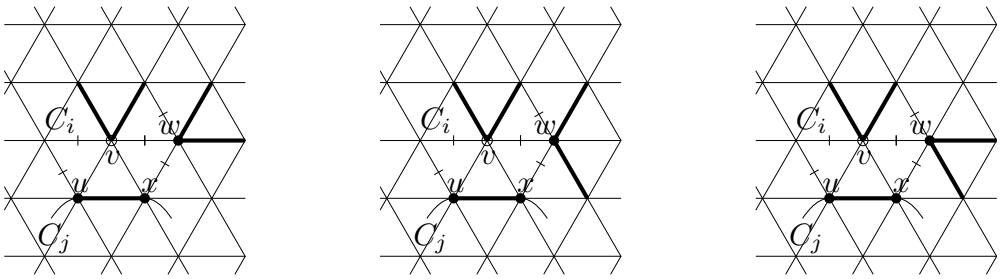

Figure 27: Different ways in which the B may go through w. Left and center: If $w \notin C_i$, we already have facing edges.

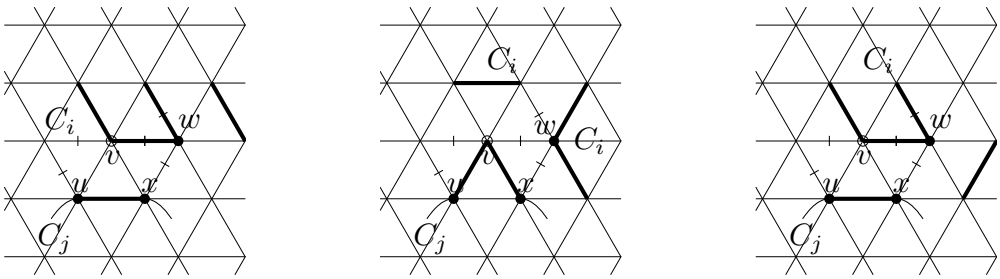

Figure 28: The modifications depending on how B goes through w in Figure 27.

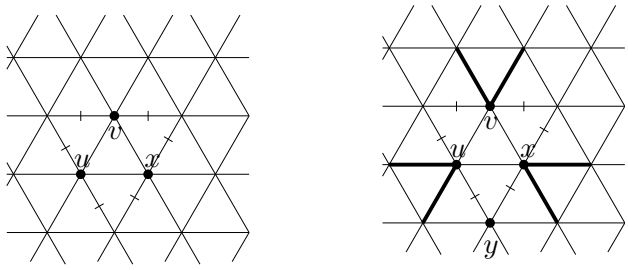

Figure 29: $C_u \neq C_v \neq C_x$.

right). Since G has no local cuts, at least one other vertex adjacent to a crossed edge is in G (in fact, at least two). Suppose $y \in G$ (Figure 29, right). Now, no matter how B visits y, we can find facing cycles. Indeed, if $y \in C_u$ or $y \in C_x$, then we are in Case I. Otherwise, the cycle to which y belongs faces both C_u and C_x.

□

Thus, starting from the boundary cycles of G, one may apply the modifications as in Lemma 3.4 and then as in Lemma 3.7 to get a Hamiltonian cycle through G.

Theorem 3.8. *Except for the Star of David (Figure 14), any polygonal triangular grid is Hamiltonian.*

A solid grid either has a cut (in which case it is not Hamiltonian), or is polygonal, Thus,

Corollary 3.9. *There exists a polynomial-time algorithm for the HCP in solid triangular grid graphs.*

4 Hamiltonian Cycles in Superthin Square Grids

In this section we prove that the HCP for superthin square grid graphs can be solved in polynomial time. We also show that in a superthin square grid there exists at most one Hamiltonian cycle. The proofs are by case analysis of the local structure of a Hamiltonian cycle.

Let $G = (V, E)$ be a superthin square grid; let $\mathcal{C}$ be a Hamiltonian cycle in G. Let $\deg(u)$ denote the degree of a vertex $u \in V$. Let v be a degree-3 vertex of G. In the figures below, vertices of G are shown with solid circles; hollow circles represent points of $\mathbb{Z}_\square \setminus V$ where there can be no vertex of G; asterisks represent grid points "in question".

Lemma 4.1. *The following statements about G and $\mathcal{C}$ are true.*

1. *There exists no degree-4 vertex in G.*
2. *$\mathcal{C}$ makes a turn at v.*
3. *There exists either a vertex of G at the grid point a, or a vertex at the grid point b, or both (Figure 30, left).*

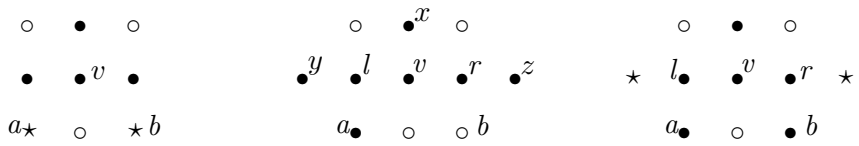

Figure 30: Left: $a \in V$ or $b \in V$. Center: $a \in V$, $b \notin V \Rightarrow (l, v) \notin \mathcal{C}$.

Figure 31: Left: $\deg(l) = 3$, $\deg(r) = 2 \Rightarrow (l, v) \notin \mathcal{C}$. Right: $\deg(l) = 3$, $\deg(r) = 3 \Rightarrow (l, v) \notin \mathcal{C}$

4. *If $a \in V$, $b \notin V$ (resp., $a \notin V$, $b \in V$) so that $\deg(r) = 2$ (resp., $\deg(l) = 2$), then $\deg(l) = 3$ (resp., $\deg(r) = 3$) and $\mathcal{C}$ goes through $r - v - x$ and $a - l - y$ (resp. $l - v - x$ and $b - r - z$) (Figure 30, center).*

5. *If $a \in V$ and $b \in V$, then at least one of l, r has degree 3 (Figure 30, right).*

6. *If exactly one of l, r (say, l) has degree 3, then $\mathcal{C}$ uses $r - v - x$ and $a - l - y$ (Figure 31, left).*

7. *If both l and r have degree 3 (Figure 31, right), then either $\deg(l') = 3$ or $\deg(r') = 3$ (or both). Thus, if there exist three-in-a-row vertices of degree 3 (like l, v, r), there exist a fourth-in-a-row vertex of degree 3 (l' or r').*

Proof. By inspection. □

Thus, in a Hamiltonian superthin grid, degree-3 vertices appear in pairs, such that the vertices in the pair are adjacent, and any Hamiltonian cycle does not use the edge between the vertices. In Figure 30, center, the pair is l, v; in Figure 31, right, the pairs are l', l and v, r (or v, r and r, r'). Whether a graph has the stated property can be checked in linear time, and hence

Theorem 4.2. *There exists a polynomial-time algorithm for the HCP in superthin square grid graphs.*

The analysis above also shows that if a Hamiltonian cycle in a superthin grid graph exists, it is unique:

Corollary 4.3. *In a superthin grid graph there exists at most one Hamiltonian cycle.*

5 Hamiltonian Cycles in Hexagonal Grids

In this section we show that the HCP for hexagonal grids is NP-complete. The grid in our reduction is polygonal, which implies hardness of the problem for polygonal hexagonal grids. Next we prove that there is a polynomial-time algorithm for the HCP in superthin hexagonal grid graphs. We do it by proving that in a superthin hexagonal grid there exists at most one 2-factor. The proof is by case analysis of the local structure of a 2-factor.

HCP for Hexagonal Grids is NP-hard

Our approach to prove hardness of the HCP for hexagonal grids is similar to the NP-completeness proofs for square and triangular grids, using a reduction from HCP in undirected planar bipartite graphs with maximum degree 3 [28]. Using the notation of Section 3, let G' be an undirected planar bipartite graph with maximum degree 3; the nodes in the parts of G' are colored "black" and "white". As before, we say the G' is composed of "nodes" and "arcs", saving the terms "vertices" and "edges" for the hexagonal grid graph G, built from G' using the following transformation.

Transformation T

1. Given G' we obtain a drawing $D(G')$ of G' as shown in Figure 32.
2. We distinguish several elements of $D(G')$, i.e., the white and black nodes, and the arcs between them. For each of these elements we provide a hexagonal grid graph that acts as a gadget that simulates the element of G'.
3. We show how to combine the gadgets culminating in the desired graph G.

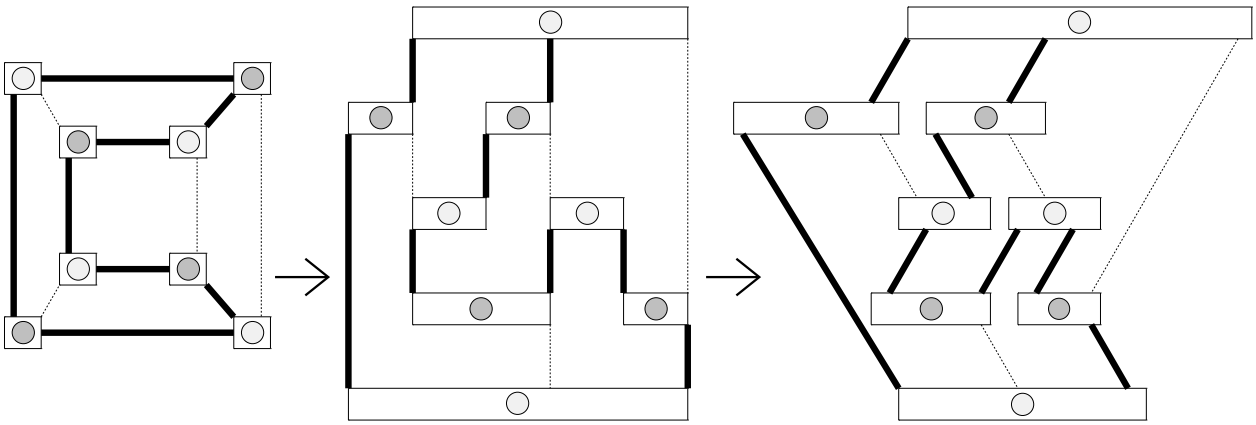

Figure 32: From left to right: a planar bipartite graph G' with maximum degree 3; planar rectilinear layout G' of G; the drawing $D(G')$. The arcs involved in an example Hamiltonian cycle are highlighted.

The details of transformation T follow.

Using methods of Rosenstiehl and Tarjan [37] or Tamassia and Tollis [38], one can obtain, in linear time, a rectilinear drawing of G' that uses a grid of linear size. We modify the drawing slightly to obtain another drawing, $D(G')$ (Figure 32), which leads to a hexagonal-grid simulation of G', the graph G. The nodes in the drawing $D(G')$ are represented by horizontal bars. The arcs of the drawing are one of two fixed angles, 60 or 120 degrees. This drawing is based on the so-called st-ordering of the nodes of G'. In an st-ordering we can choose two nodes of a face (the external face) and designate s and t the unique source and sink of a topological ordering of the graph. This ordering implies a directed acyclic structure with a single source and sink, which in the drawing

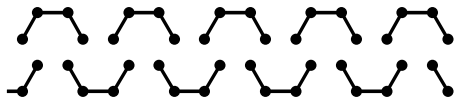

Figure 33: The tentacle.

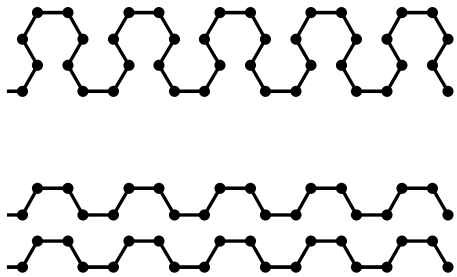

Figure 34: Tentacles with cross and return paths.

goes from top to bottom. We choose both s and t to be white nodes, as this will simplify the transformation from $D(G')$ to G. All nodes, except the nodes s and t, have at most two upward or downward arcs. The two terminal nodes, s and t, have all arcs going in the same direction. The ordering of the arcs from left to right is obtained by a compatible st-ordering of the dual graph of G' as described in [37,38]. We can convert the rectilinear planar drawing to $D(G')$ by a left to right sweep of the arcs. In this way we can draw 60-degree and 120-degree arcs and maintain planarity, which can be achieved by stretching the corresponding node bars towards the right as needed. This leads to the following lemma.

Lemma 5.1. *Given an undirected planar bipartite graph with maximum degree 3, G', we can obtain the drawing $D(G')$ in linear time.*

We proceed with the second step of our transformation, i.e., obtaining a hexagonal grid from $D(G')$. The arcs of $D(G')$ are simulated by tentacles—hexagonal strips as in Figure 33. Tentacles come in two varieties distinguished by the counter-clockwise angle made with the x-axis: 60 and 120 degrees[2]. Each tentacle can be traversed in two ways: by a cross path or a return path (Figure 34). The cross path is used to simulate an arc that is used in a Hamiltonian cycle of $D(G')$, and therefore of G', and a return path for an unused arc.

The node gadgets are made of smaller components listed below (Figure 35).

U-turn. A U-turn is used only in black nodes. The U-turn is where a return path simulating an unused arc turns back on itself. As seen in Figure 36 (left) there are two distinct ways to traverse a U-turn, one is a cross path, and the other uses two return paths.

[2]0-degree tentacles are also used as extenders inside node gadgets.

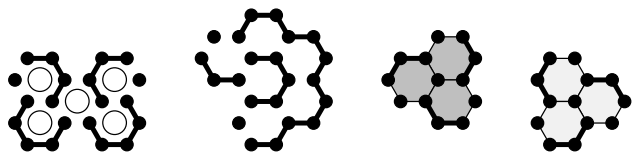

Figure 35: From left to right: U-turn, rosette, core of black nodes, and core of white nodes. The edges, used by *any* Hamiltonian cycle are highlighted.

rosette. A rosette is used to go from a horizontal tentacle to a tentacle of 60 or 120 degrees. The two ways to traverse a rosette, that is, cross and return paths, are shown in Figure 36 (middle).

core. Every node gadget has a core of three hexagons. The traversal of the core of a node gadget of degree three dictates which pair of arcs are used in a Hamiltonian cycle and which one is not. This is illustrated in Figure 36 (right). The cores of black and white nodes are reflections of each other. It is clear that given two arcs of a node, there is only one way to traverse the core.

extender. An extender is a 0-degree tentacle that is used inside the node gadgets to simulate the extent of the width of a bar from one end to the other. We use double arrows in Figure 37 to illustrate the extenders and how they can be set to any length, as the situation requires.

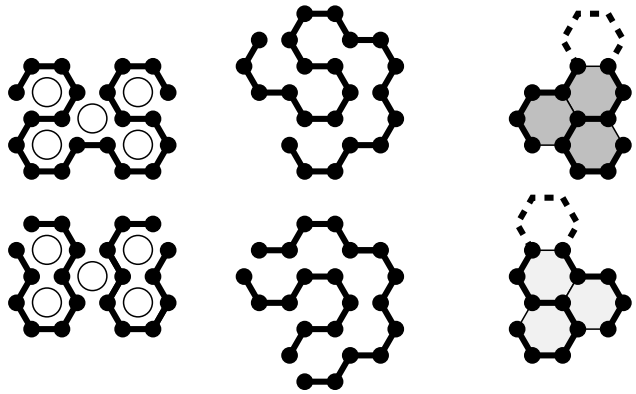

Figure 36: From left to right: U-turn, rosette, and core, with paths shown with bold lines.

We combine the components to come up with six distinct gadgets for all types of nodes. The entire collection of degree-3 node gadgets is shown in Figure 37. A degree-2 node gadget is a subset of the shown gadgets omitting all hexagons beyond the core that are associated with the third connection to a tentacle.

The last step of transformation T assembles the components to obtain the hexagonal grid G. Note that extenders can only be extended in one direction; thus, we shift the core left or right within the vertex boundary as required. A technical issue arises when trying to connect pairs of

tentacles meeting at a 60-degree angle. We only consider the tentacle-extender bends that are shown in Figure 37. This raises a parity issue, since all tentacles leaving the node gadgets need to match perfectly with each other in order to represent straight arcs. In Figure 37 we also show how this is possible for our set of node gadgets by means of an array of diagonal bands. Node gadgets are embedded in a diagonal band array, while all the tentacles are tightly enclosed within diagonal bands. Moreover, by adding or removing pairs of hexagons to the extenders, tentacles are shifted from one band to the next without skipping any. Therefore, perfect tentacle matching is guaranteed by aligning node gadgets with a predefined diagonal band array.

From Lemma 5.1, and the constructions used for the rest of transformation T, we obtain the following result.

Lemma 5.2. *Transformation T from G' to G is polynomial.*

In order to complete the proof for the NP-completeness of the HCP in hexagonal grids we need the following lemma.

Lemma 5.3. *G' is Hamiltonian if and only if G is Hamiltonian.*

Proof. (G' is Hamiltonian implies that G is Hamiltonian) A Hamiltonian cycle in G' yields a Hamiltonian cycle in G: The gadgets representing arcs in the cycle are traversed with cross paths, the rest of the arcs are picked up by return paths.

(G is Hamiltonian implies that G' is Hamiltonian) Suppose we have a Hamiltonian cycle in G. One can verify that every tentacle can be traversed in exactly one of two ways, either by a cross path, or by a return path. We now focus on the part of the cycle that passes through each node gadget. Observe that all nodes, both black and white of all degrees consist of components as shown in Figure 35 (traversed as in Figure 36), and extenders as shown in Figure 34. Each component forces one of two possible traversals, that is, cross path or return path. Thus, given a Hamiltonian cycle in G, we obtain the cycle in G': Gadgets in G that are traversed by cross paths correspond to arcs in the cycle in G. □

From Lemmas 5.2 and 5.3:

Theorem 5.4. *The HCP for hexagonal grid graphs is NP-complete.*

Observe that the grid in the proof of the above theorem is polygonal. Thus

Corollary 5.5. *The HCP for polygonal hexagonal grids is NP-complete.*

Hamiltonian Cycles in Superthin Hexagonal Grids

Let $G = (V, E)$ be a superthin hexagonal grid. A *2-factor* F in G is a 2-regular subgraph of G, i.e., a subgraph of G, in which every vertex has degree 2; in (other) words, a 2-factor is a set of vertex-disjoint cycles (of positive length) that go through all vertices.

Suppose there exist two different 2-factors, F and F', in G; suppose $v \in V$ is a vertex, visited differently by F and by F'. Clearly, v has degree 3. Given how F and F' visit v, it can be inferred

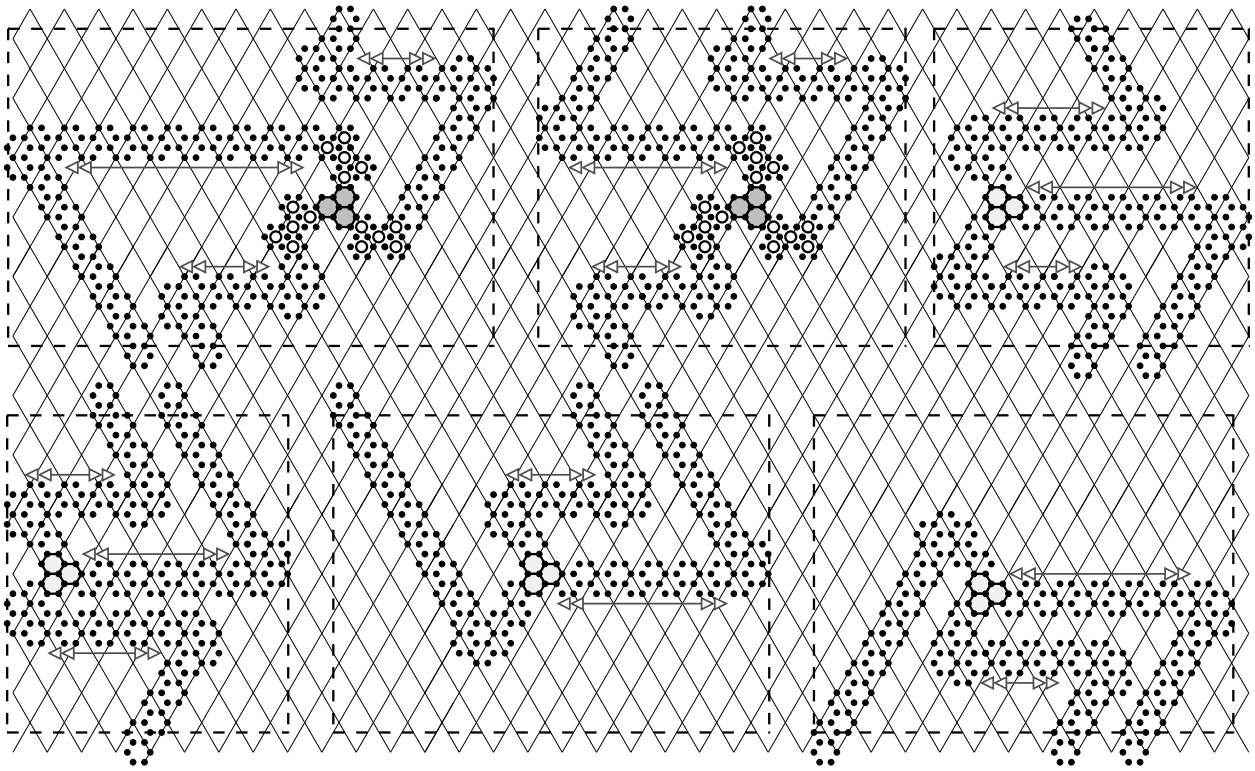

Figure 37: There are six distinct node gadgets. The anatomy of a node can be broken down to the components we call core, U-turn, extender, and rosette. These components are shown in a bounding rectangle. The core of each vertex is shaded either dark or light to represent black or white nodes respectively. Each hexagon in a U-turn is marked by a circle. At the bounding rectangle the node gadgets meet with extenders that simulate arcs. Note that the extenders are constructed so that they all fit in a diagonal band between two parallel lines. Maintaining the strips between the bands ensure that strips connecting two vertex gadgets are aligned.

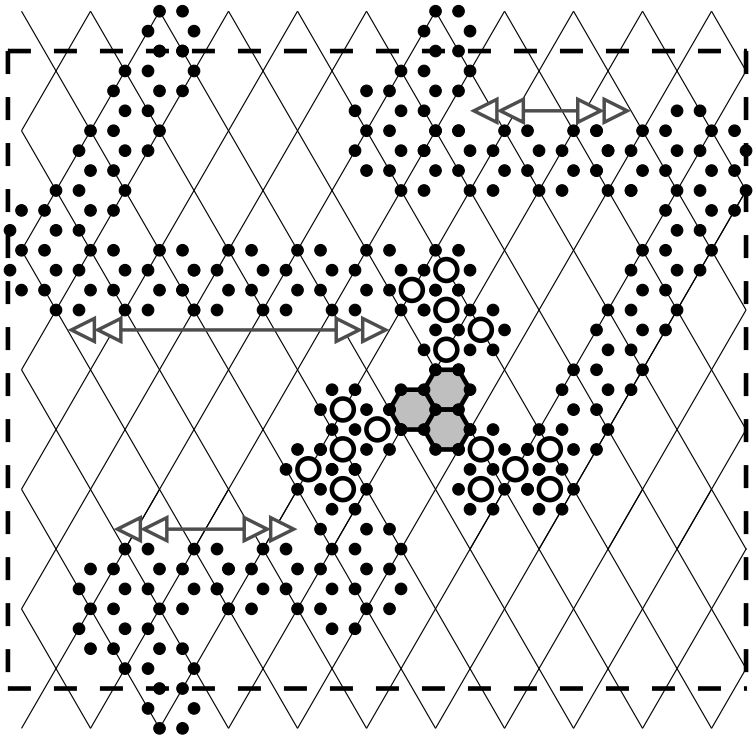

Figure 38: Top middle gadget from Figure 37.

how they visit the neighbors of v — vertices v' and v''. Refer to Figure 41. Since G is superthin, at least one of a', a'' is not in V. Indeed, otherwise both b and b'' are not in V, and both 2-factors are "stuck" at v. Say, without loss of generality, $a' \notin V$. Also since G is superthin, $w \notin V$. But then there is no way the vertex v' can be visited by F since both edges, adjacent to x, and both edges, adjacent to x', have to be used by F.

Theorem 5.6. *In a superthin hexagonal grid there exists at most one 2-factor.*

A 2-factor (if one exists) can be found in polynomial time using a b-matching algorithm [1]. Clearly, the graph is Hamiltonian if and only if the 2-factor consists of one (Hamiltonian) cycle.

Corollary 5.7. *The HCP in superthin hexagonal grids is polynomially solvable.*

6 Hamiltonian Cycles in High-Girth Graphs

By our definition (see Section 2), superthin square (resp., hexagonal) grids are the square (resp., hexagonal) grids with girth at least 6 (resp., 10). Thus, Theorems 4.2 and 5.6, and Corollaries 4.3 and 5.7 may be reformulated as follows. If the girth of a square (resp., hexagonal) grid graph G is greater or equal than 6 (resp., 10), then G has a unique Hamiltonian cycle, and it can be found in polynomial time. It seems natural to ask how general this result is, i.e., will the previous statement remain true if we drop the words "square (resp., hexagonal) grid" from it? In this section we answer

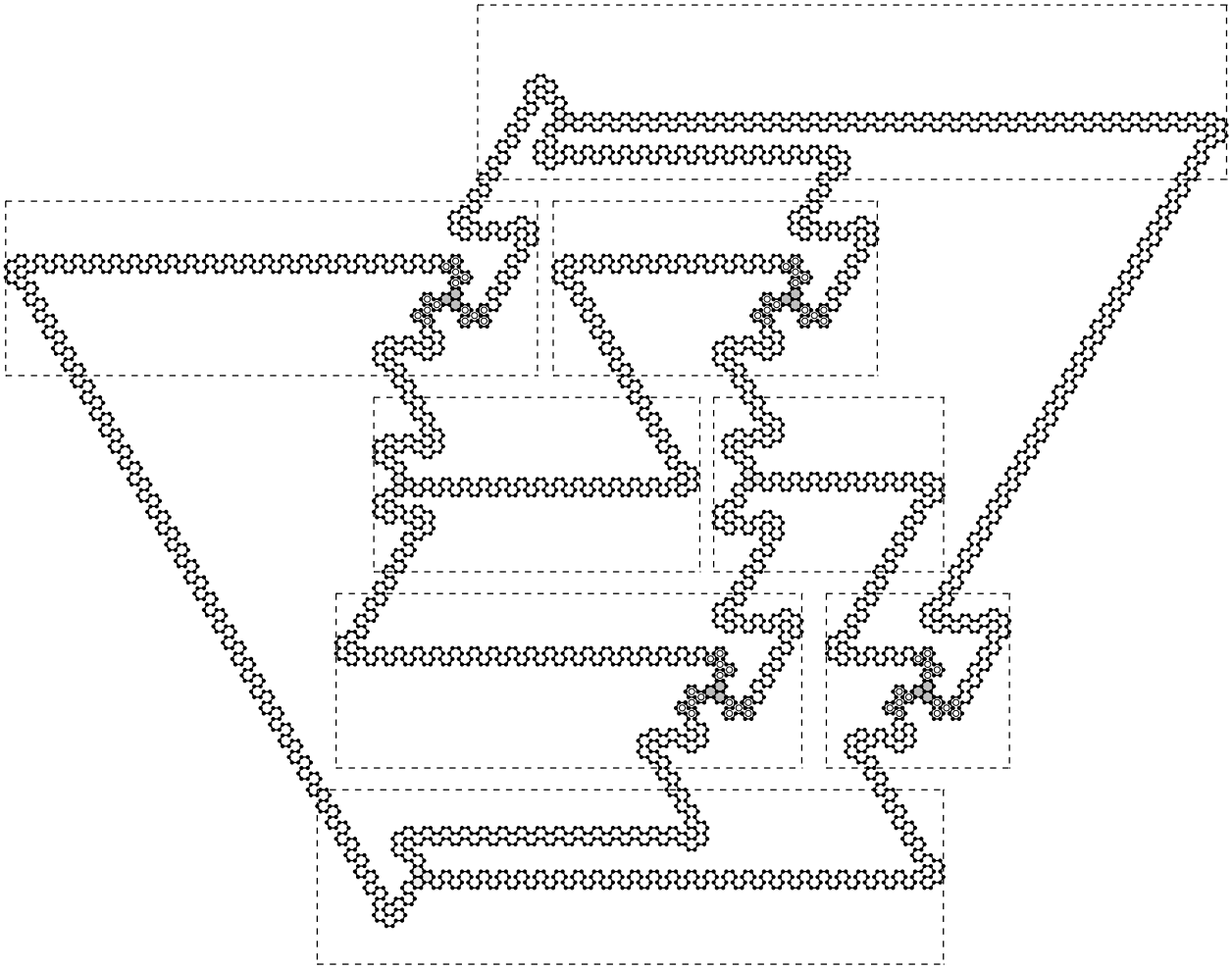

Figure 39: An example graph G that corresponds to $D(G')$ from Figure 32. A Hamiltonian cycle of G that corresponds to the Hamiltonian cycle shown for $D(G')$ has been highlighted.

the question in the negative. Specifically, we show that the HCP is hard for graphs of arbitrary girth $g \geq 6$. The problem remains hard even if restricted to planar graphs of maximum degree 3. We also show that, for any $g \geq 6, N \geq 5$, there exist planar graphs of maximum degree 3 and girth g, that have exactly N Hamiltonian cycles.

Our results come from a simple idea: Increase the girth of the hexagonal graph G from the previous section, while keeping the graph planar and subcubic, and retaining the one-to-one correspondence between the Hamiltonian cycles in it and planar bipartite subcubic graph G'.

Theorem 6.1. *For arbitrary $g \geq 6$, the HCP in planar graphs of maximum degree 3 and girth g is NP-complete.*

Proof. Let E_2 be the edges of G that are used by any Hamiltonian cycle in G (Figures. 33, 35); call these edges *black*. Replace every edge in E_2 with a path of length $g/3-2$. Make every tentacle long, so that it has at least g "wiggles" (see Figure 33). Call the resulting graph G_g. By construction,

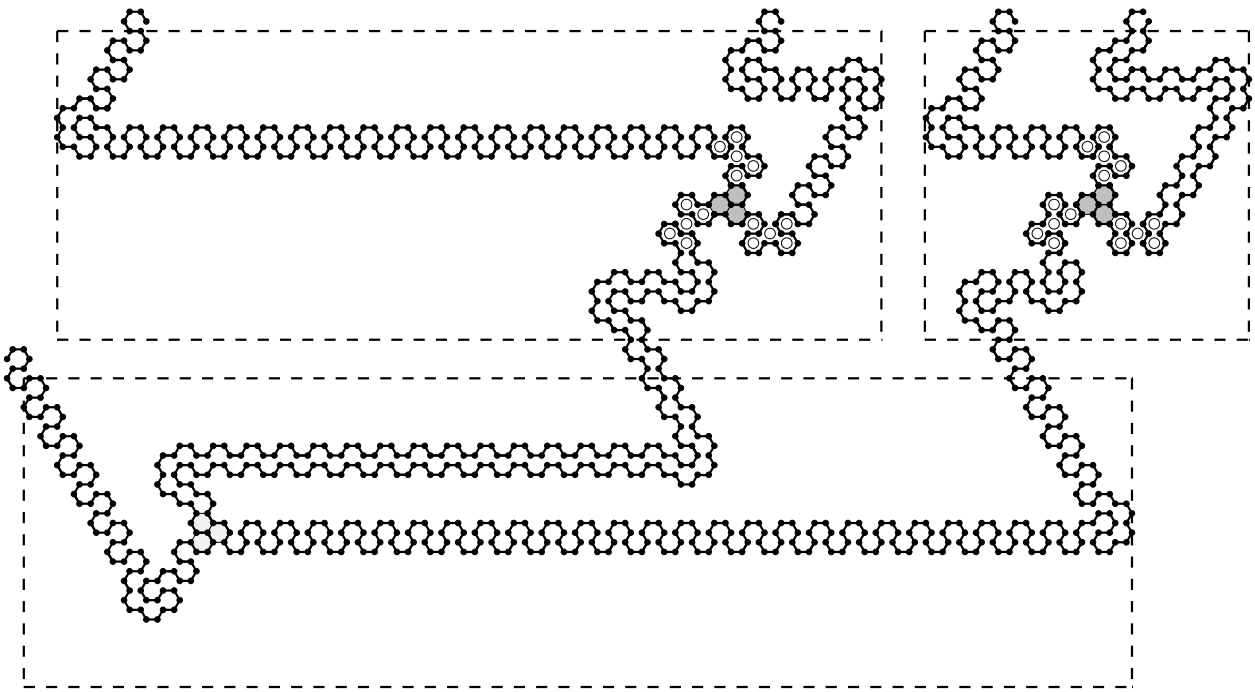

Figure 40: Bottom part of graph G shown in Figure 39.

G_g is planar and its maximum degree is 3.

Claim. *The girth of G_g is g.*

Proof. Let E_1 be the edges of G that are not black (so, call them *white*). The edges of G_g may also be called white and black: white edges are those that correspond to white edges of G, and black—those that appeared as a result of subdividing black edges of G. Any cycle in G_g that uses a black edge has length more than g (and some such cycles have length exactly g). It is not hard to see (Figures 33, 35) that any cycle within a tentacle or a node gadget has to use black edges. Finally, a cycle in G_g, consisting solely of white edges and going through two or more node gadgets, has to traverse a tentacle and thus, has length greater than g. □

Hamiltonian cycles in G_g map one-to-one into Hamiltonian cycles in G, and, thus, into Hamiltonian cycles in G'. Hence, G_g is Hamiltonian if and only if G' is. □

As a by-product of our reduction we obtain, for any $g \geq 6$, a one-to-one mapping between Hamiltonian cycles in planar bipartite graphs of maximum degree 3 and Hamiltonian cycles in planar girth-g graphs of maximum degree 3. This allows one to reason about Hamiltonian cycles in the latter in terms of the Hamiltonian cycles in the former. For instance,

Theorem 6.2. *For any $g \geq 6, N \geq 5$ there exist planar girth-g graphs of maximum degree 3 that contain exactly N Hamiltonian cycles.*

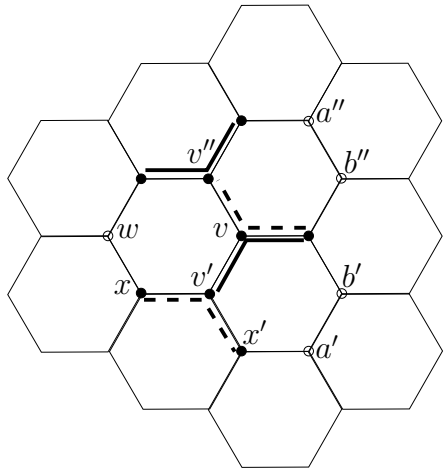

Figure 41: F is solid, F' is dashed. v is visited differently by the 2-factors; this implies how v' and v'' are visited. Since G is superthin, at least one of a', a'' is not in V. For the same reason $w \notin V$. But then F is "stuck" at v'.

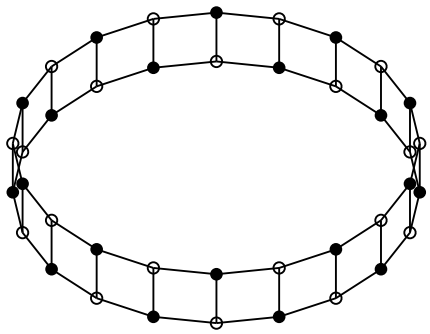

Figure 42: The prism graph $C_N \square K_2$.

Proof. The planar bipartite maximum-degree-3 (prism) graph $G' = C_N \square K_2$ (Figure 42) has exactly $N + 2$ Hamiltonian cycles (Figure 43). Thus, the high-girth graph constructed from G' by the procedure in our reduction also has exactly $N + 2$ Hamiltonian cycles. $\square$

TSP in High-Girth Graphs

The Traveling Salesman Problem (TSP) in a planar maximum-degree-3 girth-g graph has an approximation algorithm with the approximation ratio of $1 + \frac{8}{g}$. For $g > 16$ this is smaller than $3/2$, the approximation ratio of Christofides' algorithm.

Theorem 6.3. *Let G be an (unweighted) planar girth-g subcubic graph. Let T be the shortest walk that visits every vertex of G, let L be its length (i.e., the number of edges in it). Then a tour of length $(1 + \frac{8}{g})L$, visiting every vertex of G at least once, can be found in polynomial time.*

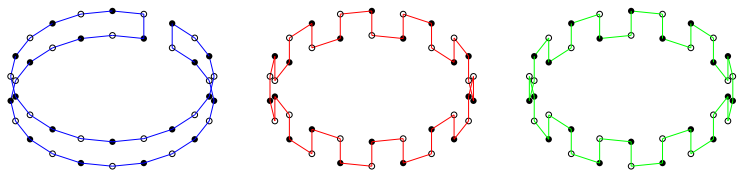

Figure 43: The Hamiltonian cycles in $C_N \square K_2$. The cycle on the left can be chosen in N different ways.

Proof. We first prove that T can be extended, to a walk that traverses every edge of G at least once, at the expense of increasing the length by at most $2d_3$, where d_3 is the number of degree-3 vertices of G. Thus, the cost of the optimal Chinese Postman tour (the tour that traverses every edge) is at most $L+2d_3$. Then, using Euler's formula, we bound $2d_3$ by $8L/g$. Because the Chinese Postman tour can be found in polynomial time, the theorem follows.

Follow T. When T passes through a degree-2 vertex, using both edges, adjacent to it, do nothing. When T passes through a degree-3 vertex, using two edges, adjacent to it, detour to visit the remaining edge, adjacent to the vertex; the cost of the detour is 2. When T makes a U-turn at a vertex v, the cost of the detour to visit the other edge(s), adjacent to v, is $2(i-1)$, where $i \in \{2,3\}$ is the degree of v. But if T U-turns at v, then there is a path to v, such that all edges along the path are traversed by T twice. Let u be the other end of the maximal such path. Clearly, u has degree 3, and all 3 edges, adjacent to it are traversed by T. Thus, the cost of adding these edges to T is 0; this amortizes the increase in the cost of adding to the tour the edges, adjacent to v.

Overall, we get a tour, traversing all edges of G, of length $L+2d_3$. Since every face of G has at least g sides, $Fg \leq 2E$, where F and E are the number of faces and edges of G. Of course, $E = d_2 + 3d_3/2$, where d_2 is the number of degree-2 vertices of G. By Euler's formula, $F = 2-(d_2+d_3)+E = 2+3d_3/2$. Thus, for $g \geq 6$, we have $2d_3 \leq \frac{4d_2+4g}{g}$. Since, clearly, $L \geq d_2$, and $L \geq g$, the theorem follows. $\square$

Remark. Having degree-1 nodes in G does not hurt the approximation factor. Indeed, the paths to the nodes must be traversed both by T and by the approximate tour.

TSP approximation algorithms with a better approximation ratio than 3/2 have been developed in several classes of graphs; refer to Table 2. However it was not always checked whether there exist examples of graphs from the corresponding classes, for which Christofides' algorithm may produce a tour longer than the proposed approximation algorithms. For the classes of graphs, studied in [4, 6, 30, 32] such examples are readily available; for the classes studied in [7, 19, 35] they are yet to be found.

Theorem 6.3 suggests another example of a class of graphs (high-girth planar subcubic graphs) for which there exists an approximation algorithm with a better performance than Christofides' algorithm. Unfortunately, as the next theorem shows, it is not possible to find a graph from the class for which Christofides' algorithm will perform worse than the Chinese-Postman-based

Class of graphs	Apx	Ref.
Solid grids	$6/5$	[4]
Geometric	$1+\varepsilon$	[6, 32]
Planar	$1+\varepsilon$	[30]
3-edge-connected cubic	$(3/2-5/389)$	[19]
Edge weights $\in \{1,2\}$	$7/5, \quad 8/7$	[7, 35]
Planar max-deg-3 girth-g	$1+8/g$	Thm. 6.3

Table 2: Approximation ratios for TSP in certain graph classes. Only for graphs from the first three classes are examples known for which Christofides' algorithm performs worse than the proposed algorithms.

algorithm from Theorem 6.3.

Theorem 6.4. *Let $G = (V, E)$ be an undirected, possibly, weighted graph. Let $Cr(G)$ (resp., $CP(G)$) be a tour produced by the Christofides' algorithm (resp., optimal Chinese Postman tour). For any structure $\mathcal{S}$ in G let $|\mathcal{S}|$ be its weight; if $\mathcal{S}$ contains an edge multiple times, the weight of the edge is counted with its multiplicity in $|\mathcal{S}|$. Then $|Cr(G)| \leq |CP(G)|$.*

Proof. For a metric ρ on V let $[G]^\rho$ denote G endowed with ρ. Let $SP(G)$ be the shortest path metric on V; we identify G with the complete graph $[G]^{SP(G)}$, called *the shortest-path metric completion* of G.

Let $MST(G)$ be a Minimum Spanning Tree of G. $CP(G)$ is obtained by adding to G a minimum-weight matching on the odd-degree nodes of G; this converts G into an Eulerian graph. $Cr(G)$ is obtained by first finding $MST(G)$ and then converting it into an Eulerian graph by adding a minimum-weight (w.r.t. $SP(G)$) matching on the odd-degree nodes of $MST(G)$. Thus,

$$|Cr(G)| \leq |CP([MST(G)]^{SP(G)})|.$$

The inequality is due to the possible "shortcuts" introduced by Christofides' algorithm (finding the best set of shortcuts is an NP-hard problem itself [34]).

$MST(G)$ is a subgraph of G, so a tour, visiting every edge in G, also visits every edge in $MST(G)$. Thus,

$$CP([MST(G)]^{SP(G)}) \leq CP([G]^{SP(G)}) = CP(G).$$

□

7 Discussion

We provided a comprehensive study of the Hamiltonian cycle problem in grid graphs. We suggested a unified classification of standard square grids and extended it to triangular and hexagonal grids. We resolved the complexity of the Hamiltonian cycle problem for many of the grid classes (see Table 1). We also addressed the Hamiltonicity of planar bounded-degree graphs with high girth.

In this section we discuss some algorithmic extensions and applications of our results. Our proof of Hamiltonicity of polygonal triangular grids (Theorem 3.8) is constructive and can be turned into an algorithm to find a Hamiltonian cycle; the algorithm runs in time linear in the number of vertices of the grid. Applying ideas from [3, 4] one can represent the cycle implicitly, so that the size of the representation is linear in the number of pixels that define the grid. The representation can be found in time linear in the number of pixels. Indeed, all that is needed to apply our modifications is to partition the grid into horizontal trapezoids. Within each trapezoid we can perform the modifications, in blocks, in $O(1)$ time. After that we are left with only $O(h)$ cycles; marching around them, we find the alternating rhombus and flip its edges.

Another feature of our modifications is that they can be done with only one pass through the grid. This is important, say, when a large triangular mesh has to be processed or displayed. A body of work in computer graphics has examined finding long cycles in triangular meshes [12–14]. We feel that the following corollary from Theorem 3.8 may have important applications.

Corollary 7.1. *Let M be a triangulated manifold containing a subgraph, on the full set of vertices, isomorphic to a triangular grid. Then, if M has no local cuts, there exists a Hamiltonian cycle through the vertices of M, and such a cycle can be found in linear time.*

Remark. Umans and Lenhart [41] observed that their algorithm for the HCP in solid square grids actually works for a larger set of graphs, quad-quad-graphs, that "locally" look like solid square grids. Corollary 7.1 is another example of a "free" extension of results for grid graphs to a more general class of graphs that locally look like grids.

Our proof of existence of girth-g graphs with a prescribed number of Hamiltonian cycles also leads to an algorithm for actually constructing such graphs. Starting from the prism graph $C_N \square K_2$, one can build the gadgets as in Section 6 in time linear in N (and g). Moreover, $C_N \square K_2$ gives a concise implicit representation of the high-girth graph.

The hexagonal grids provide better approximations to the area swept by a circular lawnmower cutter, miller, or circular vacuum cleaner. This motivates oour study of the TSP in grids that are dual to hexagonal grids, i.e., in triangular grids.

The only algorithmic work of which we are aware that used hexagonal grids for approximating the path of a circular cutter is [4]. The approximation ratio of the algorithm in [4] is $3\gamma \cdot \alpha_{TSP}$, where $\gamma \approx 1.15$ is the *dilation* of the triangular lattice, and α_{TSP} is the approximation ratio of the TSP heuristic employed. The running time of the algorithm, of course, is also dependent on the TSP heuristic, which, e.g., makes impractical the use of a PTAS [6, 32] for the TSP. Theorem 3.8 implies the following improvement to the approximation factor and running time of Theorem 3 in [4].

Corollary 7.2. *For the case of a circular cutter, the lawnmowing problem has a linear-time 3γ-approximation algorithm.*

A common technique to show that finding bounded-degree MST is NP-hard is to reduce the TSP to it. Indeed, an instance of the TSP may be reduced to an instance of the degree-k MST problem by placing a set of $k-2$ "suburbs" close to each city in the TSP; the cost of the edges

between the suburbs and between suburbs and "non-parent" cities is made prohibitively high. In [34], the degree-3 Euclidean MST problem was proved hard by reduction from the HCP (actually, Hamiltonian Path problem) in grid graphs of maximum degree 3: bounding the degree of the grid allows placing one suburb for each city in the direction of the "missing" grid vertex. The authors of [34] remarked that it did not appear possible to extend their method to show the hardness of the degree-4 Euclidean MST problem "because insertion of two suburbs [the number required for the degree-4 MST] presupposes considerably more space, and much more restrictive arrangement of the cities" [34, p. 245]. We hope that the hardness of the HCP in triangular grids of maximum degree 4 (Theorem 3.3) can potentially help here. Indeed, since the degree of each vertex in the infinite triangular grid is six, two directions around every vertex become "missing", which opens a (vague) possibility that the required two suburbs could be inserted. However, we did not succeed in finishing the argument.

Open Problems

The most natural problems left open by this work are the blanks in Table 1. In particular, what is the hardness of HCP in polygonal square grids? The grids from [11, 27, 34], used in the reductions to show hardness of HCP in square grids, have local cuts (at the "pin" connection of the tentacles to the vertex gadgets). We believe that the polynomial-time algorithm of [41] for the HCP in solid square grids can be extended to solve the HCP in polygonal square grids.

Conjecture 7.3. *HCP in polygonal square grids is in P.*

We also conjecture that the HCP in solid hexagonal grids can be solved by cycle merging, similar to what was done for the HCP in solid square grids [41].

Conjecture 7.4. *HCP in solid hexagonal grids is in P.*

An open problem, not listed in Table 1, is the hardness of the HCP in triangular grids of maximum degree 3.

A related research direction is studying the TSP in grids for which there are polynomial-time algorithms to solve the HCP. Is there a class of graphs for which HCP is in P but TSP is NP-complete?

Acknowledgments

We thank the anonymous referees for several helpful suggestions that improved the paper. We thank Andrei Antonenko, Erik Demaine, Marc Noy, and Joseph O'Rourke for discussions and comments. We thank Pavel Skums and Yury Orlovich for information on [22, 23, 33]. E. Arkin and J. Mitchell acknowledge support from the National Science Foundation (CCF-0431030, CCF-0528209, CCF-0729019), NASA Ames, and Metron Aviation. V. Polishchuk is supported in part by Academy of Finland grant 118653 (ALGODAN).

References

[1] R. P. Anstee. A polynomial algorithm for b-matchings: an alternative approach. *Inf. Process. Lett.*, 24(3):153–157, 1987.

[2] E. M. Arkin, M. A. Bender, E. D. Demaine, S. P. Fekete, J. S. B. Mitchell, and S. Sethia. Optimal covering tours with turn costs. *SIAM Journal on Computing*, 35(3):531–566, 2005.

[3] E. M. Arkin, M. A. Bender, J. S. B. Mitchell, and V. Polishchuk. The snowblower problem. In S. Akella, N. M. Amato, W. H. Huang, and B. Mishra, editors, *7th International Workshop on the Algorithmic Foundations of Robotics, WAFR*, volume 47 of *Springer Tracts in Advanced Robotics*, pages 219–234. Springer, 2006.

[4] E. M. Arkin, S. P. Fekete, and J. S. B. Mitchell. Approximation algorithms for lawn mowing and milling. *Computational Geometry: Theory and Applications*, 17(1-2):25–50, 2000.

[5] E. M. Arkin, J. S. B. Mitchell, and V. Polishchuk. Two new classes of Hamiltonian graphs. *Electronic Notes in Discrete Mathematics*, 29C:565–569, 2007.

[6] S. Arora. Polynomial time approximation schemes for Euclidean traveling salesman and other geometric problems. *Journal of the ACM*, 45(5):753–782, 1998.

[7] P. Berman and M. Karpinski. 8/7-approximation algorithm for 1,2-tsp. In *Proc. 17th Annu. ACM Sympos. on Discrete Algorithms*, 2006.

[8] A. Bjorklund and T. Husfeldt. Finding a path of superlogarithmic length. *SIAM J. Comput.*, 32(6):1395–1402, 2003.

[9] S. Bridgeman. Finding Hamiltonian cycles in grid graphs without holes, 1995. Honors thesis, Williams College.

[10] D. Briggs. Hamiltonian cycles in grid graphs without holes, 1994. Honors thesis, Williams College.

[11] M. Buro. Simple amazons endgames and their connection to Hamilton circuits in cubic subgrid graphs. *Lecture Notes in Computer Science*, 2063:250–261, 2001.

[12] A. Bushan, P. Diaz-Gutierrez, D. Eppstein, and M. Gopi. Single triangle strip and loop on manifolds with boundaries. In *Proc. 19th Brazilian Symp. Computer Graphics and Image Processing (SIBGRAPI 2006)*, pages 221–228, 2006.

[13] E. D. Demaine, D. Eppstein, J. Erickson, G. W. Hart, and J. O'Rourke. Vertex-unfoldings of simplicial manifolds. In *SCG '02: Proceedings of the eighteenth annual symposium on Computational geometry*, pages 237–243, New York, NY, USA, 2002. ACM Press.

[14] D. Eppstein and M. Gopi. Single-strip triangulation of manifolds with arbitrary topology. In *SCG '04: Proceedings of the twentieth annual symposium on Computational geometry*, pages 455–456, New York, NY, USA, 2004. ACM Press.

[15] H. Everett. Finding Hamiltonian paths in nonrectangular grid graphs. *Congressus Numerantium*, 53:185–192, 1986.

[16] T. Feder and R. Motwani. Finding large cycles in Hamiltonian graphs. In *SODA '05: Proceedings of the sixteenth annual ACM-SIAM symposium on Discrete algorithms*, pages 166–175, Philadelphia, PA, USA, 2005. Society for Industrial and Applied Mathematics.

[17] S. P. Fekete. *Geometry and the Travelling Salesman Problem.* Ph.D. thesis, Department of Combinatorics and Optimization, University of Waterloo, Waterloo, ON, 1992.

[18] H. N. Gabow. Finding paths and cycles of superpolylogarithmic length. In *STOC '04: Proceedings of the thirty-sixth annual ACM symposium on Theory of computing*, pages 407–416, New York, NY, USA, 2004. ACM Press.

[19] D. Gamarnik, M. Lewenstein, and M. Sviridenko. An improved upper bound for TSP in cubic 3-connected graphs. *Operations Research Letters*, 33:467–474, 2005.

[20] M. R. Garey, D. S. Johnson, and R. E. Tarjan. The planar Hamiltonian circuit problem is NP-complete. *SIAM J. Comput.*, 5(4):704–714, 1976.

[21] M. Ghandehari and H. Hatami. A note on independent dominating sets and second Hamiltonian cycles. (submitted).

[22] V. Gordon, Y. Orlovich, and F. Werner. Cyclic properties of triangular grid graphs. In C. P. A. Dolgui, G. Morel, editor, *Proceedings of 12th Symposium on Information Control Problems in Manufacturing (IFAC)*, volume 3, pages 149–153. A, 2006.

[23] V. Gordon, Y. Orlovich, and F. Werner. Hamiltonian properties of triangular grid graphs. Technical Report 15, Otto-von-Guericke-Universitat Magdeburg, Fakultat fur Mathematik, 2006. 22 p.

[24] R. Gould. Advances on the Hamiltonian problem — a survey. *Graphs Combin*, 19:7–52, 2003.

[25] P. Horák and L. Stacho. A lower bound on the number of Hhamiltonian cycles. *Discrete Mathematics*, 222(1-3):275–280, 2000.

[26] K. Islam, H. Meijer, Y. N. Rodríguez, D. Rappaport, and H. Xiao. Hamilton circuits in hexagonal grid graphs. In *CCCG*, pages 85–88, 2007.

[27] A. Itai, C. H. Papadimitriou, and J. L. Szwarcfiter. Hamilton paths in grid graphs. *SIAM J. Comput.*, 11:676–686, 1982.

[28] D. S. Johnson and C. H. Papadimitriou. Computational complexity. In E. L. Lawler, J. K. Lenstra, A. H. G. Rinnoy Kan, and D. B. Shmoys, editors, *The Traveling Salesman Problem*, pages 37–85. John Wiley & Sons, New York, 1985.

[29] R. Karp. Reducibility among combinatorial problems. In R. Miller and J. Thatcher, editors, *Complexity of Computer Computations*, pages 85–103. Plenum Press, 1972.

[30] P. N. Klein. A linear-time approximation scheme for tsp for planar weighted graphs. In *Proceedings, 46th IEEE Symposium on Foundations of Computer Science*, pages 146–155, 2005.

[31] V. K. Leontiev. Hamiltonian cycles in torical lattices. In *Proceedings of EUROCOMB*, 2005.

[32] J. S. B. Mitchell. Guillotine subdivisions approximate polygonal subdivisions: A simple polynomial-time approximation scheme for geometric TSP. *k-MST, and related problems, SIAM J. Comput.*, 28:1298–1309, 1999.

[33] Y. Orlovich, V. Gordon, and F. Werner. Hamiltonian cycles in graphs of triangular grid. *Doklady NASB*, 49(5):21–25, 2005. (In Russian).

[34] C. H. Papadimitriou and U. V. Vazirani. On two geometric problems related to the Traveling Salesman Problem. *J. Algorithms*, 5:231–246, 1984.

[35] C. H. Papadimitriou and M. Yannakakis. The traveling salesman problem with distances one and two. *Math. Oper. Res.*, 18(1):1–11, 1993.

[36] V. Polishchuk, E. M. Arkin, and J. S. B. Mitchell. Hamiltonian cycles in triangular grids. In *Proceedings of the 18th Canadian Conference on Computational Geometry (CCCG'06)*, pages 63–66, 2006.

[37] P. Rosenstiehl and R. E. Tarjan. Rectilinear planar layouts and bipolar orientations of planar graphs. *Discrete Comput. Geom*, 1:343–353, 1986.

[38] R. Tamassia and I. G. Tollis. A unified approach to visibility representations of planar graphs. *Discrete Comput. Geom*, 1:321–341, 1986.

[39] A. G. Thomason. Hamiltonian cycles and uniquely edge colorable graphs. *Ann. Discrete Math.*, 3:259–268, 1978.

[40] C. Thomassen. On the number of Hamiltonian cycles in bipartite graphs. *Combinatorics, Probability & Computing*, 5:437–442, 1996.

[41] C. Umans and W. Lenhart. Hamiltonian cycles in solid grid graphs. In *Proc. 38th Annu. IEEE Sympos. Found. Comput. Sci.*, pages 496–507, 1997.

[42] C. M. Umans. An algorithm for finding Hamiltonian cycles in grid graphs without holes, 1996. Honors thesis, Williams College.